ACS OMEGA

Open Access

This article is licensed under CC-BY-NC-ND 4.0

http://pubs.acs.org/journal/acsodf

Article

Fossil-Free Polyethylene and Polypropylene Production via CCU and Biomass Pathways: A Harmonized Techno-Economic Assessment

Shiyu Ding, Gert Jan Kramer, André Faaij, Juliana Garcia Moretz-Sohn Monteiro, and Matteo Gazzani*

Cite This: *ACS Omega* 2026, 11, 4314−4332

Read Online

ACCESS | Metrics & More | Article Recommendations | Supporting Information

ABSTRACT: The transition to a fully sustainable chemical industry requires new technologies and value chains, where fossil fuels are replaced as both energy source and carbon feedstock. To identify the key metrics that will make the transition viable, we developed a modeling framework for techno-economic assessment and applied it in a case study of co-manufacturing polyethylene and polypropylene from sustainable sources of carbon, viz. captured carbon utilization and biomass pathways. Differently from existing literature, our modeling framework bridges user-defined economic parameters, thermodynamic-based process models, and process performance assessment consistently throughout the different pathways. In this manner, the process designs and economic assessment are harmonized in assumption and scope, enabling a fair, detailed comparison. The results indicate that the optimal pathway depends on the specific performance metric under consideration: cost, energy efficiency, or carbon efficiency. The biomass pathway via ethanol is the most cost-effective at around 1,500−3,000 EUR/t_{PP+PE}, the biomass pathway via gasification route is the most energy-efficient at 32%, while the carbon capture and utilization pathway exhibits the highest carbon efficiency—64%, or up to 83% when including secondary products. Last but not least, details of our thermodynamic-based process models and costing method are provided, addressing the harmonization of our results and delivering portable results to other studies.

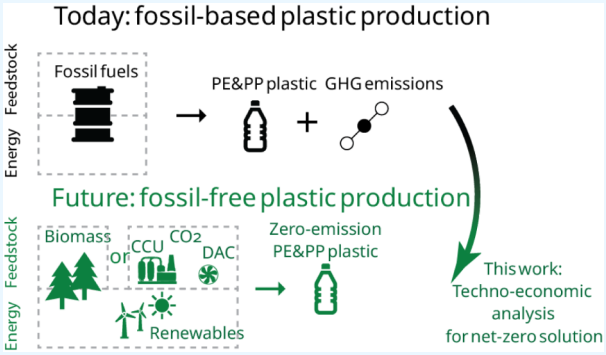

INTRODUCTION

The net-zero transformation of the chemical industry is challenging because fossil fuels provide both energy and carbon feedstocks. While the energy transition, especially in the electricity sector, has been facilitated by growing renewable capacity, the reduction of CO_2 emissions in the process and chemical industries has not yet gained momentum. Three main system barriers can be identified: fossil-free chemical industries need new process designs and new value chain designs, which are typically mutually dependent; defossilized chemical processes struggle to access affordable fossil-free carbon feedstock and hydrogen; last but not least, large-scale validation of new process designs and new technologies requires large initial capital investments, and moreover, the production of fossil-free products is hardly economically competitive without carbon taxes.[1] In addition, technical challenges exist, in particular with the supply of high-temperature process heat.[2] Technology assessment and system-level conditions (e.g., costs, value chain, feedstock availability) are typically brought together in techno-economic assessment (TEA).

More specifically, TEA is pivotal for the identification of the key metrics required to proceed with the field demonstration, which, in the chemical industry, is particularly capital-intensive. Not surprisingly, literature on TEA abounds.[3−5] Overall, we can distinguish between two different types of analyses. On the one hand, there are detailed, thermodynamic-based assessments that typically utilize specific process models and computer-aided process software to calculate energy and mass balances. Similar analyses are most commonly used to assess specific technologies and optimize particular technology configurations. Several examples can be found in the literature on climate-driven technologies. van der Spek et al. found that capturing CO_2 from industrial flue gas was more economical using chemical absorption with a monoethanolamine solvent than by using membranes;[6] Poluzzi et al. assessed the techno-economic performance of converting biomass into methanol or hydrogen via biomass gasification;[7] Anicic et al. compared the cost of direct methanol synthesis and indirect methanol synthesis;[8] and Ortiz-Espinoza compared the techno-economic performance of oxidative coupling of methane and methanol-to-olefins processes to convert shale gas to ethylene.[9] Given

Received: September 16, 2025
Revised: October 23, 2025
Accepted: October 31, 2025
Published: January 14, 2026

© 2026 The Authors. Published by American Chemical Society

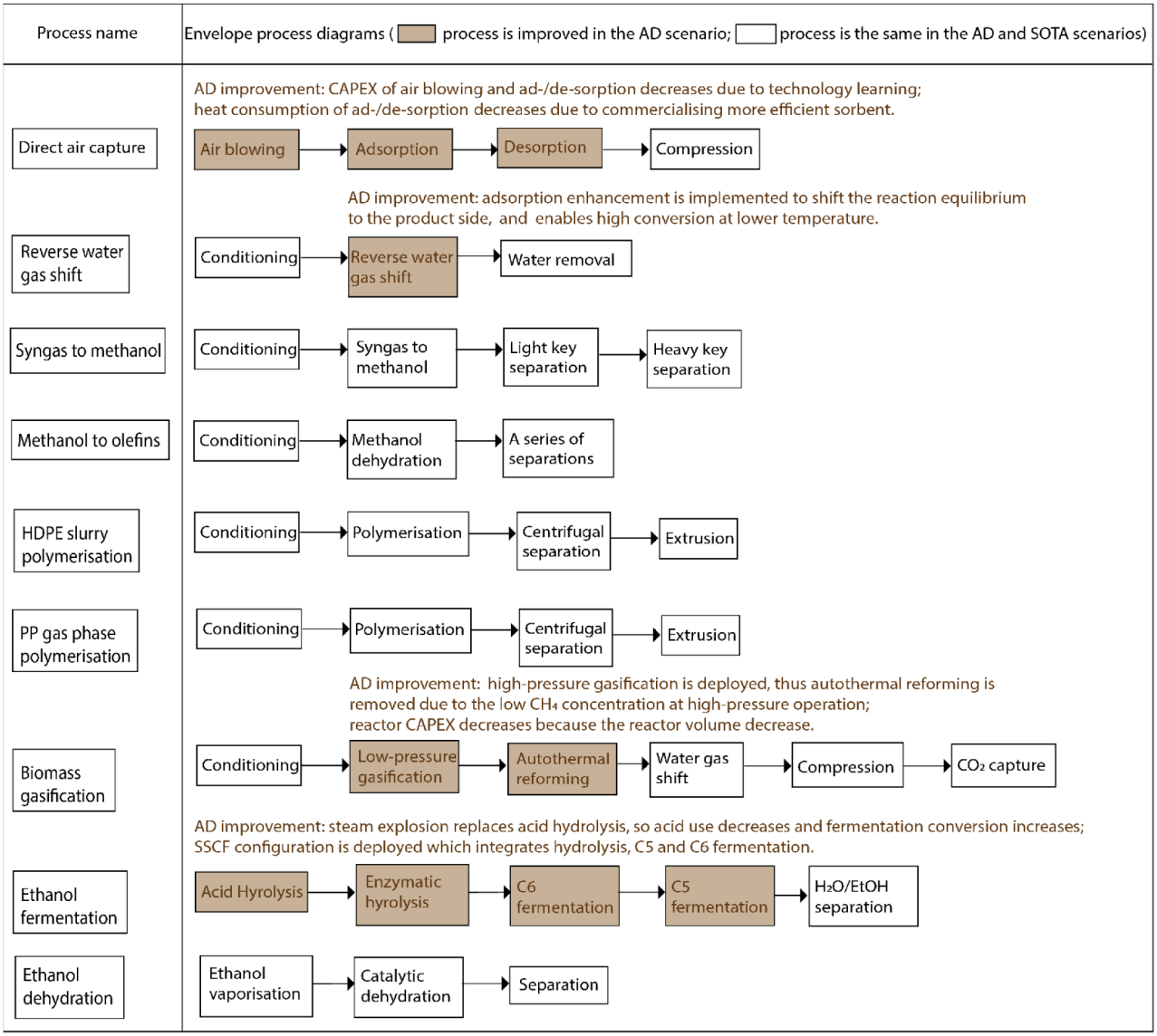

Figure 1. EPD of process models in the SOTA and AD scenarios: the brown boxes indicate improved processes in the AD scenario, and the black boxes indicate that the processes in the SOTA and AD scenarios are the same.

the narrow scope of technology-specific TEAs, similar analyses hardly cover the entire value chain from feedstock to the final product, resulting in the exclusion of the potential influence of process configuration changes on downstream and upstream processes. On the other hand, higher-level TEAs with input/output models are commonly used to compare several solutions or evaluate scenarios; these typically rely on performance data from literature and investigate the role of system boundaries on technologies. Voldsund et al. and Gardarsdottir et al. collected data from detailed TEA studies to compare different technologies for CO_2 capture in cement plants.[10,11] Zhao et al. compared different routes for ethylene production in China,[1] and Allgoewer et al. evaluated the cost and emissions of converting CO_2 captured from air into valuable chemicals.[12] System-level TEAs have a broad scope and allow comparison of different technology pathways. However, using high-level data collected from different works that adopt different methods and tools reduces the quality of the technical assessment while also introducing possible inconsistencies and additional sources of uncertainty. More specifically, while the calibration of economic assumptions and scales is commonly achieved, the calibration of process design (e.g., methods, reactor configuration), equipment cost correlations, and computation of key performance parameters is not commonplace in system-level TEA.

This analysis remains valid when looking specifically at the transition toward a fossil-free chemical industry, especially in the context of carbon-based products and, as a particularly relevant end product, plastics. TEAs are either technology-specific[13,14] or built upon literature process models.[15] The work by Uekert et al. and Hernández et al. are valuable exceptions, where multitechnology comparisons are carried out using process models; however, both works remain limited in scope, with the former focusing on closed-loop plastic recycling and the latter focusing on depolymerization routes.[16,17]

With this work, we aim to (i) provide a new, comprehensive, harmonized techno-economic analysis of different pathways for the production of high-density polyethylene and polypropylene starting from nonfossil feedstock; and (ii) go beyond the

https://doi.org/10.1021/acsomega.5c09670
ACS Omega 2026, 11, 4314−4332

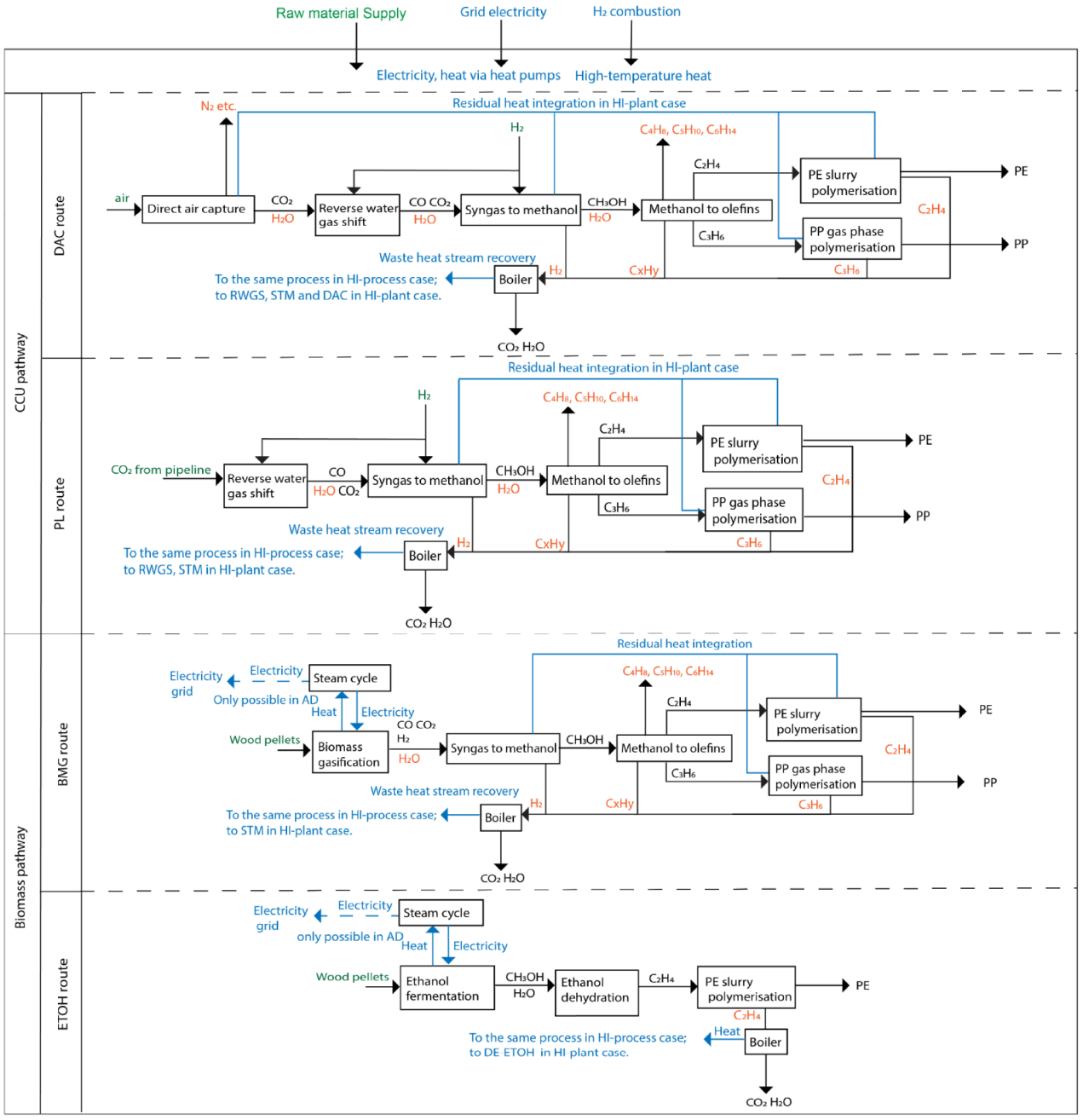

Figure 2. Process connection, material flow, and heat integration network (HEN) configuration of assessed routes: reverse water gas shift is abbreviated to RWGS; syngas to methanol is abbreviated to STM; direct air capture is abbreviated to DAC; and ethanol dehydration is abbreviated to DE-ETOH.

common TEA approach by bridging detailed process modeling and economic assessment for several inherently different processes. Accordingly, we include biobased (BIO) routes as well as carbon capture routes from air and concentrated sources, comparing the performance of the different routes under different scenarios. In order to do that, we develop a modular modeling framework enabled by computer-aided process modeling for simultaneously designing and assessing different comprehensive fossil-free pathways based on their techno-economic performance, scoped from feedstock to final product. All process models and assessments are performed with the same simulation platform, which maintains consistency in assumptions, design parameters, and equipment cost correlations. In addition, the modeling framework is designed to be flexible in terms of economic parameter input and process model connection, making it adjustable or portable to other studies. We take polyethylene (PE) and polypropylene (PP) as a case study, as they are widespread, global chemical products that are comanufactured at large scale.[18] Moreover, to the best of our knowledge, the analysis of different fossil-free routes to produce PE and PP is missing in the current literature. Specifically, two comanufacturing pathways for polyethylene (PE) and polypropylene (PP) are designed and assessed: one where carbon is provided by CO_2 capture and one where biomass is used. For each pathway, two different process routes are assessed: direct air capture and

https://doi.org/10.1021/acsomega.5c09670
ACS Omega 2026, 11, 4314−4332

pipeline for CO_2 capture and gasification and ethanol for biomass. We discuss the key performance indicators (KPIs) of fossil-free PE and PP manufacturing, including energy consumption, carbon efficiency, carbon emissions, and cost. Furthermore, we consider the uncertainties of the KPIs arising from potential technology development, heat integration levels, energy mix, and material prices.

PROCESSES FOR PRODUCTION OF FOSSIL-FREE PE AND PP

To produce fossil-free PE and PP, carbon feedstocks can be sourced from CO_2 captured from nonfossil sources (including from air) or directly processed from biomass; we hereafter refer to these two pathways as CCU and BIO pathways, respectively. While various conversion processes can be adopted within each pathway, in this work, we focus on those closest to commercialization, i.e., approximately those having a technology readiness level (TRL) higher than 5. The Envelope Process Flow Diagram (EPD) in Figure 1 shows the different subprocesses selected in this work for the two pathways, along with high-level details of the different building blocks per process. Figure 2 shows instead the full production processes from feedstock to product. The CCU pathway includes: (a) CO_2 sourcing, (b) reverse water gas shift, (c) syngas to methanol, (d) methanol to olefins, and (e) polymerization. The BIO pathway includes: (f) biomass gasification, (g) ethanol fermentation, and (h) ethanol dehydration; moreover, processes (c)-(d) are needed in the case of biomass gasification. Polymerization is present in all cases. It is worth noting that we explore two different performance levels: the first represents the state-of-the-art (SOTA), where the different processes perform according to the current technology availability; the second includes expected technology advancements (AD) for critical units, i.e., where future performance might deviate substantially from the SOTA. These include direct air capture, reverse water gas shift, gasification, reforming, hydrolysis, and fermentation.

Moreover, we consider two different scenarios for heat integration. In one case, heat integration is only allowed at the process-level, hereafter referred to as *HI-process*; the HI-process case does not allow for cross-process heat integration. In the second case, an additional heat network is built at the plant level. Therefore, in the HI-plant, both cross-process and process-level heat integration can be achieved. An overview of investigated cases is provided in Table 1.

The processes of the selected pathways are assembled from feedstocks to final PE−PP products and are designed in MATLAB and ASPEN Plus (see Section Methodology: modeling framework). In the following, we discuss in more detail the different specific routes to understand what technologies can be adopted, also with respect to the SOTA and the advanced technology development scenario. The following description provides a first overview of the technologies and processes, and the interested reader can refer to the Supporting Information for more details on reactor designs and operating conditions.

PE and PP Production with Carbon Capture and Utilization

The CCU pathway starts with the provision of carbon feedstock (CO_2), which can either be captured from the air or purchased from point sources and transported via pipelines. This, therefore, defines two different routes, both of which are considered in the analysis: the *DAC route* and the Pipeline route (or *PL route*). When the two routes are compared, the PL route excludes the energy-intensive DAC process and consequently demands less energy (and is likely cheaper), but its feedstock might not be available if the pipeline infrastructure is not close to the production site or if the point-source CO_2 is in shortage after the phasing out of fossil fuels. It is worth noting that the PL route does not necessarily translate to fossil-free PE and PP; certainly, there is the possibility that CO_2 in the pipeline has fossil origins. However, this point is out of scope for the present work, where we exclusively focus on plant and process levels. On the other hand, the DAC route concentrates CO_2 directly from the air, and therefore has no direct fossil emissions. After CO_2 is provided to the system, it is first reduced to CO in the reverse water-gas shift (RWGS) reactor and further converted into methanol in the syngas-to-methanol (STM) reactor. Methanol can be dehydrated into different olefins, which become the feedstocks for other processes, or it is combusted for heat recovery. The PL route, starting with concentrated CO_2 instead of the dilute CO_2 stream, features different compression designs, syngas compositions, and heat exchange networks (HENs) compared to the DAC route. Otherwise, the processes are equivalent.

Table 1. List of the Investigated Cases

Pathway	Route	Tech. development	HEN level	Label
CCU	DAC	SOTA	Process	DAC-HI-process-SOTA
			Plant	DAC-HI-plant-SOTA
		AD	Plant	DAC-HI-Plant-AD
	PL	SOTA	Process	PL-HI-process-SOTA
			Plant	PL-HI-plant-SOTA
		AD	Plant	PL-HI-Plant-AD
BIO	BMG	SOTA	Process	BMG-HI-process-SOTA
			Plant	BMG-HI-plant-SOTA
		AD	Plant	BMG-HI-Plant-AD
	ETOH	SOTA	Process	ETOH-HI-process-SOTA
			Plant	ETOH-HI-plant-SOTA
		AD	Plant	ETOH-HI-Plant-AD

The two CCU pathways are illustrated in Figure 2, including process connections, material flows, and plant-level heat exchange network (HEN) configurations.

DAC. The DAC process has two main technology pathways at TRL 6−7, distinguished by sorbent types:[19] solid sorbent- and liquid sorbent-based processes. In comparison, solid sorbent shows lower energy consumption and higher productivity than liquid sorbent, and for this reason, solid sorbent is selected in the model.[20] The solid-sorbent DAC process consists of air blowing, adsorption at ambient conditions, and desorption at ca. 100 °C; moreover, compression is added to provide CO_2 at the state required by the downstream process (PFD is shown in SI Figure 12). For the design and performance of DAC and CO_2 compression, we adopt values from the literature. In the SOTA scenario, we consider values from the TEA report from the National Energy Technology Laboratory (NETL), with a heat consumption of 6.15 MJ/kg CO_2.[21] In the AD scenario, we consider a significant decrease in heat consumption: as shown in Sabatino et al., the heat consumption can potentially be reduced to 3.8 MJ heat/kg CO_2 by using MCF-APS-hi sorbent.[20] A significant cost decrease of DAC is also expected

https://doi.org/10.1021/acsomega.5c09670
ACS Omega 2026, 11, 4314−4332

by the International Energy Agency (IEA), as considered in the AD scenario, through technology learning at a learning rate of 15%, resulting in the CAPEX (excluding compression CAPEX) declining by 62% by 2030.[22] These predictions might, in fact, be very optimistic and prove very difficult to materialize; yet, we prefer to be technology-optimistic in the AD case.

Pipeline CO_2. The PL CO_2 input is rather straightforward. However, depending on the point source and pipeline characteristics, PL CO_2 may vary in pressure level and impurities.[23] For the sake of simplicity in our model, the PL CO_2 stream is assumed to be purchased at high purity (approximately 100%) and 25 bar, meaning the PL CO_2 stream is ready to be used on-site for syngas production.

RWGS. The RWGS process reduces CO_2 into CO thermocatalytically at high temperatures (600−1000 °C) and preferably high pressures (<30 bar) to reduce equipment volume and CAPEX. In this work, we model the RWGS process in ASPEN Plus with an approach to equilibrium based on pilot plant.[24] We consider supplying the high-temperature heat via imported H_2 while other routes might be viable, e.g., electrification. H_2 entails limited changes compared to current technologies. The main equipment includes tubular reactors, heat exchangers, and flash drums (the PFD in the SOTA scenario is shown in SI Figure 13, and the PFD in the AD scenario is shown in SI Figure 14). RWGS is currently at around TRL 7, and the industrialization of this process is limited by sourcing CO_2 and developing stable catalysts under high reaction temperatures.[24] One solution being investigated, and therefore considered in the AD scenario, is the sorbent-enhanced RWGS (SERWGS) process, which decreases the reaction temperature to 350 °C thanks to the shift in equilibrium achieved by removing the products, more precisely by adsorbing water.[25] Thanks to the decreased reaction temperature, the heat for supporting the reactor can be more easily sourced, for example, by a simpler electric boiler, resulting in a cheaper reactor. However, the SERWGS process requires extra sorbent recovery, which leads to increased energy consumption and cost. Additionally, the SERWGS process has a different product composition than the RWGS process, requiring the redesign of the downstream processes.

STM. The STM process is a mature commercial process, which is described in detail, for example, in Ullmann's Encyclopedia.[26] The reaction is carried out at 50−100 bar and 200−300 °C, and distillation columns are used to separate methanol from water, gases, and other alcohols (PFD in SI Figure 15). Although the process design for such a commercial process is well established, the heat consumption is reported differently in the literature, ranging from heat neutral to 4.58 MJ/kg methanol (details seen in SI Section 2.3). In addition, the syngas feedstock in a fossil-free route differs from the conventional syngas produced via the steam methane reforming (SMR) process. According to the reaction stoichiometry, the conventional feed stream has a molar composition at H_2:CO:CO_2 = 3:1:0.33, while the feed composition is 3.3:1:0.43 in the RWGS process and 2:1:0 in the SERWGS process (SI Figure 13 stream table and SI Figure 14 stream table). Tuning the syngas composition by removing CO_2 in the RWGS/SERWGS process to match the conventional syngas composition will increase energy consumption and CAPEX; in contrast, maintaining a high concentration CO_2 feed lowers the STM reaction kinetics because increased water formation leads to poorer catalyst performance, thereby increasing the CAPEX of the STM process. Building kinetic models may help determine the optimal syngas composition, but that would require a detailed reactor design, which is beyond the scope of this study. Therefore, we model the STM process at equilibrium without optimizing syngas composition.

MTO. There are two main technology options for MTO, namely, syngas-to-dimethyl-ether-to-olefins (SDTO) and direct methanol-to-olefins (DMTO). In this work, we select DMTO because of its superior economic performance.[27] MTO is a mature technology; here, we adopt the design parameters and the process performance data as reported by Chen et al.[28] It is worth noting that multiple products are produced in the MTO process (see Figure 16 in the SI), including ethylene, propylene, other light olefins, and byproducts. C_2H_4 and C_3H_6 are polymerized into plastic pellets as key products in the process; other light olefins are allocated based on their economic value at the current light olefin price (SI Price Excel file). Additional byproduct streams are assumed to be combusted for heat recovery because of their low flow rate and complex composition.

Polymerization. Ethylene and propylene are polymerized into PE and PP pellets (PPE and PPP processes). The feedstock is of high purity, and the polymerization process is commercial. Process design details are reported in SI Sections 3.5 and 3.6; the processes are implemented in Aspen Plus.

Heat Network. The details of the process-level HEN are presented in the process flowsheet diagram (PFD) provided in the Appendix. When looking at the plant-level HEN, it should be noted that the STM and the MTO processes produce low-caloric-value waste fuels that can be burned to provide high-temperature heat. This is, therefore, used to cover all of the heat demand of the reverse water gas shift. The remaining heat is used in the ethylene polymerization and propylene polymerization processes. Moreover, the STM has additional heat available from product cooling; reusing this makes PPE and PPP fully heat-integrated. As for the remaining heat, the HEN design depends on the source of CO_2: in the DAC route, since the separation of CO_2 from air is heat-intensive but requires low temperature, waste heat can be conveyed to the DAC unit. However, a net heat demand for DAC remains. Although the HEN in the HI-plant case is more energy-efficient than the HI-process case, constructing all the processes in one location may be challenging regarding infrastructure construction, labor sourcing, and utility supply.

PE and PP Production from Biomass

In the BIO pathway, the carbon feedstock enters the plant as carbon bound in biomass. Among the various types of biomass, wood pellets are selected in our study because they are comparatively abundant, do not compete with the food supply, are available on the market, and are easy to transport. Accordingly, the BMG and ETOH routes are designed to convert wood pellets into PE and PP with high selectivity.

The BMG route is suitable for feeding with softwood pellets that have a high caloric content and are easy to ignite. As shown in the conversion steps in Figure 2, wood pellets are first gasified into syngas, which is then converted into methanol. Methanol is dehydrated into olefins, including ethylene and propylene, which are polymerized into PE and PP. Most of the process layout in the CCU pathway can be reused in the BMG route by adjusting operating parameters. The biomass gasifier represents the largest process difference.

Whereas the ETOH route is suitable for poplar wood pellets as feedstock, which have high cellulose and hemicellulose

https://doi.org/10.1021/acsomega.5c09670
ACS Omega 2026, 11, 4314−4332

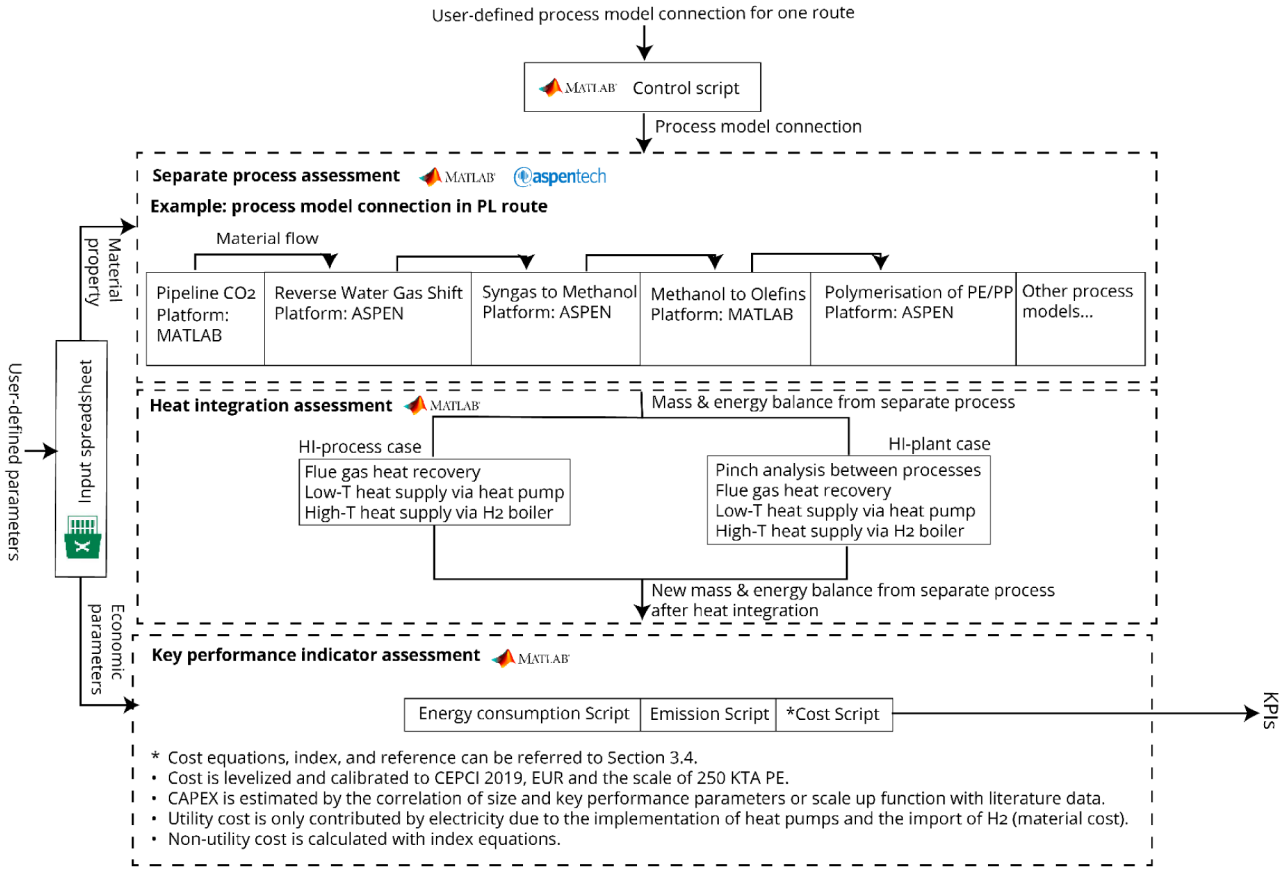

Figure 3. Modeling framework scheme with functional modules and the input/output flow.

content for achieving a high yield of ethanol, the conversion steps from wood pellets to plastics are presented in Figure 2. Poplar wood pellets can be hydrolyzed and fermented into ethanol (ETOH process), which is then catalytically dehydrated into ethylene (DE-ETHOH process) and processed into PE.

Biomass Gasification. The gasifier converts carbonaceous biomass into gas upon reaction with gasification agents (air, O_2 and steam) under high temperature and preferably high pressure (the detailed PFDs for the SOTA and AD scenarios are shown in SI Figures 23 and 24). Biomass gasification is at TRL 6−7, and there are already several pilot plants, e.g., a 140 MW plant in Vassa.[29−31] The key challenges include gasifier design and its continuous operation. Different gasifiers are reported in the categories of direct, indirect, fixed bed, fluidized bed, and entrained flow reactor; these are compared in SI Table 15.[32] Considering the TRL, the scaling-up ability, and the efficiency, a low-pressure circulating fluidized bed gasifier from Foster Wheeler at 4.5 bar (operational) is selected in the SOTA scenario, while a high-pressure bubbling fluidized bed reactor at 25 bar (exit) from GTI is instead selected in the AD scenario. The higher pressure reduces the methane content and the reactor volume, lowering the total costs.[7,33] For the reaction, wood pellets are co-fed with steam and oxygen to achieve high energy efficiency. The remaining process design changes with the composition and pressure level of raw syngas; the gasification is followed by syngas cleaning to remove char and dust, which is critical to the energy efficiency of the process. To this end, we select a ceramic filter process because of its low-pressure drop at high temperature (max. 600 °C).[34] After cleaning, syngas typically has a molar ratio of H_2:CO $+CO_2$ at around 1, while 2−3 is required for methanol synthesis. To meet this requirement in this system, carbon capture and autothermal reforming (ATR) are used. Given that the ATR converts carbonyl sulfide and other organic sulfur compounds into H_2S, sulfur purification is placed downstream.[35] The rest of the BMG route shares the same design as the CCU pathway. Several process design differences are introduced when moving from the SOTA to the AD design; most notably, the ATR is not needed because CH_4 concentration in the raw syngas is low, thereby affecting the syngas compression energy and the upgrading steps. Overall, this leads to a lower CAPEX and lower energy consumption in the AD scenario.

ETOH Fermentation. The ethanol route differs substantially from the CCU and BMG ones. Here, we consider a second-generation ethanol process, where lignocellulosic biomass is used as feedstock. Compared to the first-generation sugars-based process, this has the key advantage of not competing with food production. The second-generation process has been commercialized, but the deployment is limited to a few plants. Therefore, the optimal process configuration is still a matter of debate, mainly with respect to the pretreatment process and reactor integration.[36] In both the SOTA and the AD designs (the PFDs of both are taken from existing NREL reports,[37,38] hydrolysis of hemicellulose in lignocellulosic biomass (first) and of cellulose (second) takes place. These are followed by C6 and C5 fermentation and ethanol purification. The differences between SOTA and AD are introduced at the reactor level: for SOTA, we consider a

https://doi.org/10.1021/acsomega.5c09670
ACS Omega 2026, 11, 4314−4332

commercial plant design with dilute acid pretreatment and separate hydrolysis and fermentation (SHF). For the AD scenario, several advanced technologies are available at the pilot-plant scale, which are reported in SI Table 30. We selected steam explosion and simultaneous saccharification and cofermentation (SSCF) because of the reduced acid consumption and increased integration degree, respectively. To deal with the various feedstock compositions and pretreatment technologies, specific fixed fermentation yields were assumed for each chemical component (e.g., glucan, xylan, lignin) of the feed.

ETOH Dehydration. The DE-ETOH process dehydrates ethanol into ethylene. The commercial process includes vaporization, catalytic dehydration (300−500 °C) and separations, as described in detail by Frosi et al.[39,40] Yet, questions remain open, such as, whether to remove water before or after the dehydration reactor: while the presence of water hinders the reaction on the product side, separation after the reaction is easier. In industry, ethanol is typically requested with a purity of 95%;[40,41] yet, the performance of the ethanol dehydration reactor with high water content is uncertain. Here, we take the conservative approach of conventional ethanol dehydration with separation before the reaction.

Heat Network. The HEN of the BMG route in the HI-plant case is designed as follows: the residual heat from the STM process can be integrated by heat exchangers with the processes of PPE and PPP in the HI-plant case, resulting in heat neutrality for the PPE and PPP processes. The waste heat streams from the processes of STM, MTO, PPE, and PPP can be combusted for heat recovery to reduce the heat demand in the STM process. As for the HEN of the ETOH route, the only integration possibility between different processes is to combust the waste heat stream from PPE, which is used in the PPE process in the HI-process case and in the DE-ETOH process in the HI-plant case. In addition, residual heat from the BMG or ETOH processes is converted to electricity via steam cycles, and the assessment result shows that there is excessive electricity sold to the grid, apart from supplying the BMG and ETOH processes in the AD scenario.

METHODOLOGY: MODELING FRAMEWORK

The modeling framework developed for the harmonized assessment of CCU and BIO PE/PP production makes use of different software platforms: Excel for data input, Aspen Plus V12.1 for process modeling, and MATLAB R2021a for process modeling and overarching techno-economic calculations. The scheme illustrated in Figure 3 provides an overview of the modeling framework, which consists of (i) a control script, (ii) process models, (iii) a plant-level heat integration script, (iv) a key performance indicator assessment script, and (v) a user-defined input sheet. The framework logic is as follows : The control script in MATLAB sequentially calls different process models as identified by the connections in the full plant layout; input/output stream information is stored in MATLAB and transferred to the next process model. Process models are designed to cope with a certain degree of flexibility in scale and feedstock composition by defining the correlations between economic performance and process design parameters with input changes in the script, so that the models can be used in different routes. The resulting mass and energy balances and the equipment performance of each process are input to the assessment module, which calculates heat integration potential, total energy consumption, costs, carbon efficiency, and emissions. In addition, the assessment model enables automatic sensitivity analysis, for example, of economic parameters defined by the user.

Key Economic Parameters

The key economic parameters used in this study are listed in Table 2. For simplicity, we assume that all production routes (feedstocks to products) are located in the Netherlands, and the costs are reported in 2019 EUR. A sensitivity analysis on feedstock price is included here to provide additional guidelines. In terms of energy demands and costs, we consider:

- Low-temperature heat is provided by heat pumps, where the CAPEX increases with the required temperature level, the utility OPEX depends on the electricity price and electricity consumption, and the nonutility OPEX is fixed as shown in Section Key performance indicator assessment;
- High-temperature heat is supplied by H_2 boilers assuming H_2 is purchased at a fixed market price and the boiler's CAPEX is the same as conventional gas boilers. While we acknowledge that hightemperature electrification is also a viable route for high temperature heat, it would require ad hoc design for every reactor type, whereas combustion is closer to current industrial practice; we therefore adopt a more conservative combustion-based approach

Table 2. Key Economic Assumptions and Parameters

Economic Parameter			
Location		The Netherlands	
Reference year		2019	
Plant lifetime		25 years	
Plant capacity		250 KTA PE	
Discount rate		10%	
Material	Price (EUR/t)	Reference	Range (EUR/t)
Pipeline CO_2[a]	100	ETS[42]	
Electrolysed H_2[b]	4650	IEA[43]	[840 5930]
Wood Pellets[c]	162	Market review[44]	[81 243]
Energy	Price (EUR/kWh)	Reference	Range (EUR/kWh)
Electricity-grid-2019-NL[d]	0.065	Market review[45]	[0.01 0.10]
Conversion CAPEX	Price (MEUR/MW)		Reference
Gas boiler[e]	0.054		46
Heat pump[f]	0.72−1.03		46

[a]Pipeline CO_2 is assumed to be available at the required pressure (25 bar in our model) and 100% purity. [b]The lower and higher price of electrolyzed H_2 is assumed to be determined by the electricity cost with the price range [0.01 0.10] EUR/kWh and 60% electrolysis efficiency. [c]The price of wood pellets is assumed to be within the range of ±50% of the referenced price. [d]The average electricity price in 2019 in the Netherlands is used, associated with the emission factor in Table 5. [e]The boiler CAPEX cost 0.055 MEUR/MW in the reference in 2020. After CEPCI (chemical engineering plant cost Index) calibration, the reference cost is 0.054 MEUR/MW. [f]The heat pump CAPEX depends on the output temperature. The reference reported the CAPEX of 80 °C heat pump CAPEX is 0.73 MEUR/MW in 2020; 120 °C for 0.87 MEUR/MW; 150 °C for 1.05 MEUR/MW. As with the boiler, the result after calibration is 0.72−1.03 MEUR/MW.

https://doi.org/10.1021/acsomega.5c09670
ACS Omega 2026, 11, 4314−4332

Table 3. Platform of Process Models and Key Assumptions of Modelling

Process	Software platform	Key process assumption
DAC	Simplified simulation in MATLAB, with compression in Aspen Plus	Modular technology with constant performance at different scales (scale up factor is 1).
RWGS	Aspen Plus	Equilibrium simulations. SOTA: reaction reaches equilibrium at 900 °C and 25 bar; AD: sorption enhanced RWGS process reaches equilibrium at 350 °C and 25 bar with water removed from the products. Reactor is difficult to scale up.
STM	Aspen Plus	Reaction reaches equilibrium at 80 bar and 250 °C; the reactor can process CO:CO_2 feedstock at the molar ratio higher than 1.
MTO	MATLAB	Fixed input/output, with scale up factor of 0.67
PPE	Aspen Plus	Ziegler−Natta kinetic schemes
PPP	Aspen Plus	Ziegler−Natta kinetic schemes
BMG	Aspen Plus	The process is continuous; yield model to replicate experimental syngas composition, which is kept fixed at different scales.
ETOH	MATLAB	Fixed conversion for each chemical composition of biomass.
DE-ETOH	MATLAB	The water content in feedstock does not influence the ethylene yield.

Process Modules

Process models are built in Aspen Plus, Matlab+Aspen Plus, and Matlab. We use the first case when we aim to have a detailed process simulation that can consistently assess the process performance under varying conditions (e.g., reforming, WGS). Matlab is instead used for simpler process assessment, where we do not expect deviations from the basic process conditions (e.g., methanol to olefins). The model type for all key processes is shown in Table 3. Interested users can find additional information for each process type, including a decision tree for model selection, in the SI.

Heat Integration

In this work, we consider heat integration within each process (both in HI-process and HI-plant cases) and across different processes at the plant level (only in the HI-plant cases). The computation of heat integration is carried out both directly in the Aspen Plus flowsheets and in dedicated MATLAB scripts according to the following possible cases:

- Residual heat reused within a process: heat integration is computed by directly designing heat exchangers in Aspen Plus;
- Residual heat across processes: heat integration is computed with a plant level pinch analysis carried out in a dedicated Matlab script;
- High-temperature heat from combustion of byproducts and fuel gases: heat is recovered at process and plant level and computed using a dedicated Matlab script;
- Heat pumps for low-temperature heat (below 155 °C) and H_2 boilers for temperature above 155 °C are simulated as simple input/output models in a dedicated Matlab script.

The integration step, the system boundaries, and the heat source are depicted in Figure 3; the heat exchange parameters and energy conversion efficiency are shown in Table 4.

Key Performance Indicator Assessment

In this work, we consider technical, environmental, and economic key performance indicators: (i) specific energy and heat consumption, (ii) carbon efficiency, (iii) specific CO_2 emissions, and (iv) levelized cost of PE and PP. In the following, we discuss in more detail how these are computed.

The specific energy consumption is provided as (i) direct specific electric consumption in the full process, i.e., excluding the energy required for H_2, (ii) direct heat consumption in the full process; moreover, we provide the overall energy input to the full process when also considering H_2 import (PL/DAC cases) and biomass import (BMG/ETOH cases).

Table 4. Parameters for Heat Integration

Stream phase	Pinch temperature (K)	Reference
Liquid−liquid	5	Assumed
Gas−liquid	10	Assumed
Gas−gas	15	Assumed
Process	Efficiency	Reference
Heat pump	60% of Carnot efficiency[a]	Deutz et al.[47]
Gas boiler	85% of LHV	Assumed
Steam cycle efficiency	35%	Poluzzi et al.[48]

[a] $\eta_{Carnot} = \frac{T_h}{T_h - T_l}$

The process energy efficiency is calculated as a first-law efficiency, given by the ratio between the energy in the products and the total input energy, as defined in eq 1,

$$\eta_{PE+PP} = \frac{\dot{m}_{PE}\cdot LHV_{PE} + \dot{m}_{PP}\cdot LHV_{PP}}{\dot{m}_{H_2}\cdot LHV_{H_2}/\eta_{H_2} + \dot{W}_{electricity} + \dot{m}_{BM,dry}\cdot LHV_{BM,dry}} \quad (1)$$

where η_{PE+PP} is the energy efficiency of fossil-free PE and PP production, η_{H_2} is the H_2 electrolysis efficiency (60%), and $\dot{W}_{electricity}$ is the process electricity consumption

Carbon efficiency and CO_2 emissions are calculated based on the mass and energy balance from process models. The carbon efficiency is a simple accounting of how carbon is redistributed throughout the full system; therefore, it stems directly from the overall mass balances. On the other hand, CO_2 emissions are computed starting from the electricity and hydrogen inputs to the plant. Given that we consider starting from CO_2-neutral carbon[1], emissions are associated exclusively with the emission rate of the electricity grid, which is also considered for the production of hydrogen. While we do not directly incorporate H_2 production in process models, we believe reporting emissions from grid-connected electrolyzers is needed to provide a complete picture of the system, calculate the required electricity needs, and associated emissions. Given the variety and decreasing trend in the grid electricity emission factor, we performed a sensitivity analysis ranging from zero

https://doi.org/10.1021/acsomega.5c09670
ACS Omega 2026, 11, 4314−4332

(total green) to the emission factor of grid electricity in the Netherlands in 2019 Table 5.

Table 5. Emission Factor

Source	Emission (kg CO_2/kWh)	Reference	Range (kg CO_2/kWh)
Electricity-grid-2019-NL	0.37	Government report[49]	[0 0.37]

The levelized cost of PP and PE is calculated using bottom-up CAPEX, OPEX, annualization factors, and economic allocation to consider multiple products. The total cost of manufacturing fossil-free PE and PP is determined by summing CAPEX, utility OPEX, and nonutility OPEX. The CAPEX is scoped as the total plant cost (TPC), which includes equipment purchase cost, installation cost, contractor services cost, contingency cost, etc.[50] Specifically, for the process model developed in MATLAB, we calibrate the CAPEX and OPEX data from the literature using the Chemical Engineering Plant Cost Index (CEPCI) (eq 2), currency adjustments, economic assumptions, and scaling-up functions (eq 3). For the process models developed in Aspen Plus, we use the equipment key performance parameters from the process models to estimate the equipment purchase cost, which is then multiplied by the Lang factor to obtain the TPC (e.g., 4.74 for fluid processes), as shown in eq 4. Then, eqs 5 and 6 are used to annualize CAPEX. Nonutility OPEX is calculated as shown in eq 7 and utility OPEX is calculated as shown in eq 8. All the equations for CAPEX and OPEX calculations are referred to in the textbook by Peters et al.[51] The CAPEX correlation equations are formulated with the principle that more extreme conditions or larger sizes lead to more expensive equipment, while nonutility OPEX includes different categories that are proportional to fixed capital investment, operating labor cost, and utility cost. Regarding the final component, utility OPEX is only contributed by electricity. The total cost is then allocated using economic allocation factors for secondary products, using eq 9, and the results are presented after being levelized by the summed production rate of PE and PP with eq 10. The cost calculation is summarized in Figure 3.

$$\mathrm{EPC}_{2019} = \mathrm{EPC}_{\text{reference year}} \cdot \frac{\mathrm{CEPCI}_{2019}}{\mathrm{CEPCI}_{\text{reference year}}} \tag{2}$$

$$\mathrm{EPC}_A = \mathrm{EPC}_B \cdot \left(\frac{\mathrm{Capacity}_A}{\mathrm{Capacity}_B}\right)^{f_{\text{scale up}}} \tag{3}$$

where, EPC: equipment purchase cost; A: equipment/plant at current scale; B: equipment/plant at referred scale; $f_{\text{scale up}}$: scaling-up factor. The value given in the reference is used; for modular technology such as DAC, 1 is used; otherwise, 0.67.

$$\mathrm{TPC} = \sum^{\text{all equipment}} f_{\text{Lang}} \cdot \mathrm{EPC} \tag{4}$$

where, TPC: total plant cost.

$$f_{\text{annualization}} = \frac{r(1+r)^T}{(1+r)^T - 1} \tag{5}$$

where, $f_{\text{annualization}}$: capital annualization factor; r: discount rate; T: lifespan of the plant.

$$\text{annualized CAPEX} = \mathrm{TPC} \cdot f_{\text{annualization}} \tag{6}$$

$$\text{non-utility OPEX} = 0.16 \cdot \mathrm{FCI} + 2.41 \cdot C_{\text{operating labour}} + 0.09 \cdot C_{\text{utility}} + C_{\text{material}} \tag{7}$$

where, C: cost; FCI: fixed capital investment.

$$\text{utility OPEX} = \mathrm{P}_{\text{electricity}} \cdot \mathrm{W}_{\text{electricity}} \tag{8}$$

where, $\mathrm{W}_{\text{electricity}}$: annual electricity consumption.

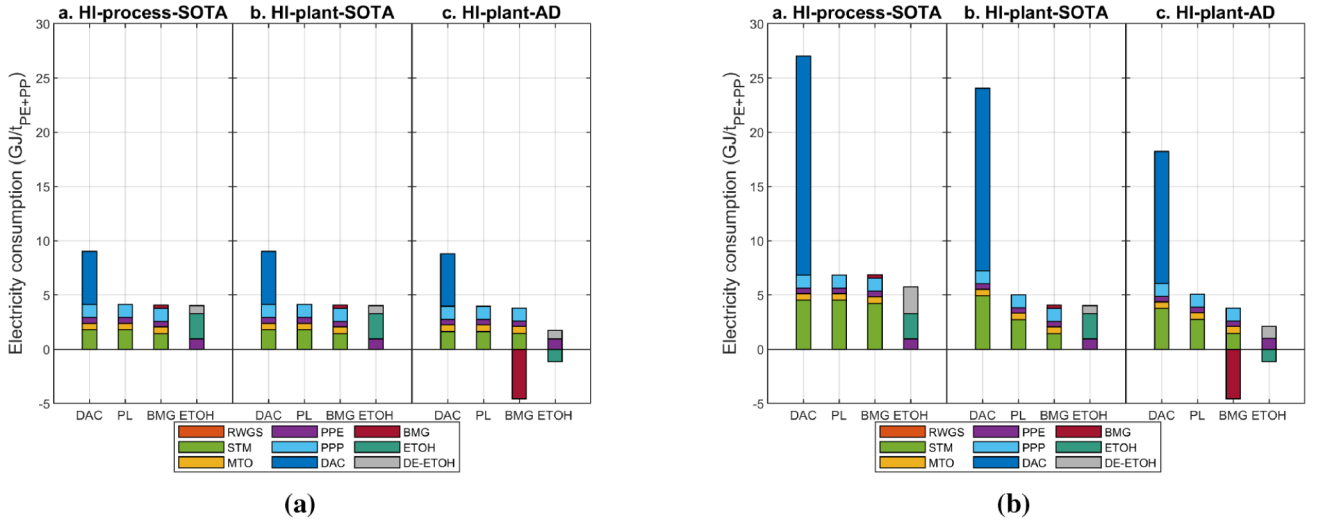

Figure 4. Specific electricity consumption for PE+PP for the 12 different cases considered in the paper (DAC, PL, BMG, and ETOH for HI-process-SOTA/HI-plant-SOTA/HI-pant-AD). The total electricity consumption is broken down into the different processes and color-coded as shown in the legend. (a) Direct electricity consumption, i.e., excluding electricity for H_2 production and heat pumps. For the biomass cases (BMG and ETOH), the electricity consumption shown here already includes the balance between consumption and production from valorisation of the biomass byproducts and the electricity generated via the steam cycle for recovering residual heat. (b) Indirect electricity consumption including electricity for heat pumps, which provide low-temperature heat.

https://doi.org/10.1021/acsomega.5c09670
ACS Omega 2026, 11, 4314−4332

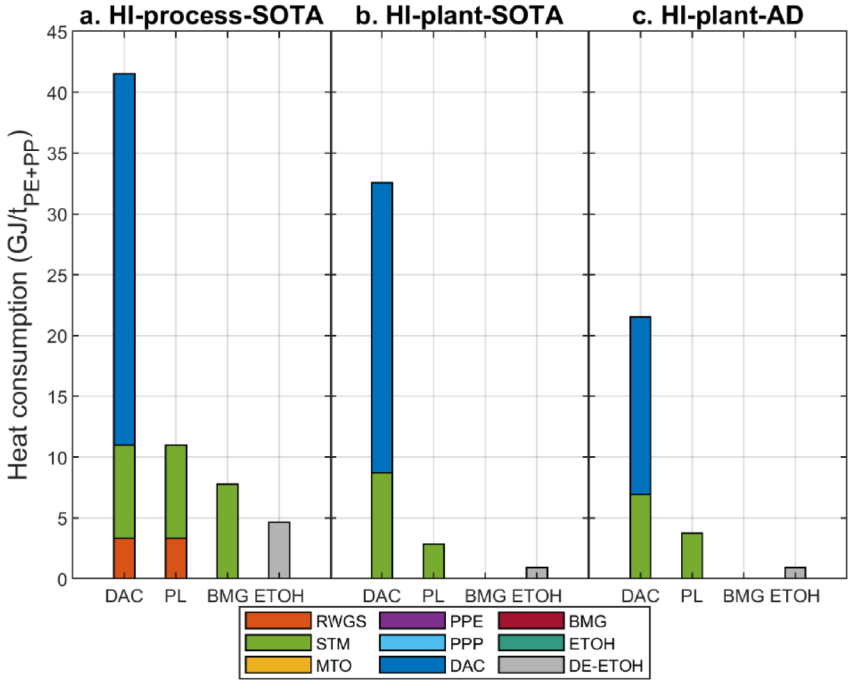

Figure 5. Specific direct heat consumption for PE+PP for the 12 different cases considered in the paper (DAC, PL, BMG, ETOH for HI-process-SOTA/HI-plant-SOTA/HI-pant-AD), including the low-temperature heat supplied by heat pumps. The total heat consumption is broken down into the different processes and color-coded as shown in the legend.

$$f_{\text{econ,PE+PP}} = \frac{m_{PE}\cdot P_{PE} + m_{PP}\cdot P_{PP}}{m_{PE}\cdot P_{PE} + m_{PP}\cdot P_{PP} + \sum_{j\neq PE,PP} m_j\cdot P_j} \quad (9)$$

where, $f_{\text{econ,PE+PP}}$: economic allocation factor of PE and PP.

$$C_{PE+PP} = [f_{\text{econ,PE+PP}}\cdot \sum^{\text{All process}} \text{annualized CAPEX} + \text{Non-utility OPEX} + \text{Utility OPEX}]/(m_{PE} + m_{PP}) \quad (10)$$

where, C_{PE+PP}: levelized cost of PE and PP

RESULTS OF TECHNO-ECONOMIC ASSESSMENT

Four fossil-free PE and PP manufacturing routes are designed and assessed using the modeling framework introduced in Section Methodology: Modeling Framework: DAC, PL, BMG, and ETOH routes. Moreover, three cases are developed per route to evaluate the role of plant-level heat integration and technology performance. In the following, we discuss and compare the cases based on the different KPIs introduced above: energy consumption, energy and carbon efficiency, and levelized costs of PP and PE. We would like to stress that the figures and tables presented in the following section are complemented by detailed mass and energy balances per process in the Supporting Information file.

Energy Consumption

The energy (electricity and heat) consumption is presented for manufacturing one tonne of fossil-free PE and PP via the considered pathways and scenarios, respectively, in the form of both direct and indirect consumption. As illustrated in Figure 4, the indirect electricity consumption is considerably higher than the direct electricity consumption, attributed to the implementation of heat pumps for low-temperature provision. The heat pump implementation also almost depletes the direct heat consumption (shown in Figure 5)

Comparing the four routes, the DAC route has the highest direct electricity consumption (8.8−9.0 GJ/t_{PP+PE}); this is due to the high volume of air to be processed and the high compression duty required to provide the requested carbon feedstock. Therefore, air blowing and compression of the CO_2 as a DAC product result in around 5 GJ/t_{PP+PE} directly. The other three routes consume a similar amount of direct electricity, around 4 GJ/t_{PP+PE}. It is worth noting that there are no significant changes in the direct electricity consumption between the HI-process-SOTA and the HI-plant-SOTA cases, as plant-level heat integration does not bring a reduction in direct electricity consumption in the processes. On the other hand, reductions are achieved when introducing technology advancements compared to the state-of-the-art (HI-plant-AD case): DAC and many other processes become more efficient. The largest difference is found in the biomass cases. In the SOTA route, power consumption in the gasification island is substantially similar to the power production from high-temperature surplus heat, resulting in 4.6 MW of electricity needed for the gasification island (135.9 MW requested vs 131.3 produced—see Table 22 of SI); in the AD route, power production is substantially larger than the power needs (78.2 MW requested vs 153.2 MW produced—see Table 26 of SI), resulting in a net export of power from the gasification island to the rest of the plant. This is enabled by high-pressure biomass gasification, which significantly reduces the syngas compression duty. Similar trends are found for the ETOH route, where technology advancement decreases direct electricity consumption because of the energy-efficient pretreatment and reactor integration; in this case, the fermentation island becomes a net power producer instead of a net power consumer. As a result, BMG and ETOH routes in the AD case have almost neutral direct electricity consumption,

https://doi.org/10.1021/acsomega.5c09670
ACS Omega 2026, 11, 4314−4332

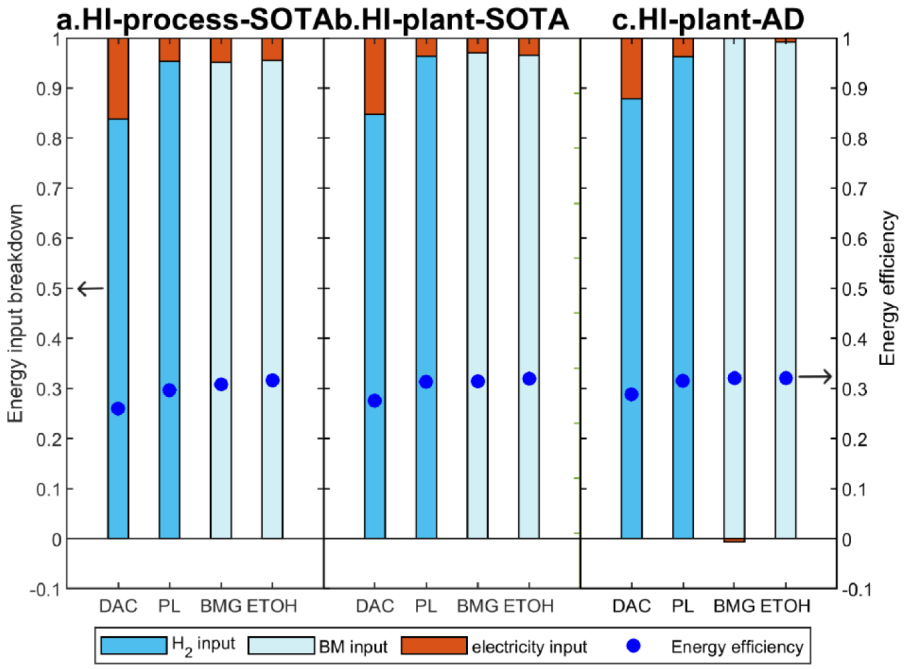

Figure 6. Energy input breakdown (shown in bar) and energy efficiency (shown in dots) for the 12 different cases considered in the paper (DAC, PL, BMG, ETOH for HI-process-SOTA/HI-plant-SOTA/HI-pant-AD). The energy input is contributed by both material (electrolyzed H_2 and woody biomass) and process energy supply, and the energy efficiency represents the ratio of the product energy output to the energy input.

i.e., electricity production in the process compensates almost entirely for the consumption. In conclusion, it is worth stressing that technology development is effective in reducing process electricity consumption for the BIO pathway but not for the CCU pathway.

Similarly to the direct electricity consumption, the direct heat consumption of the CCU pathway is higher than that of the BIO pathway (see Figure 5). As expected, the DAC route shows the highest direct heat consumption in all three cases (21.55−41.53 GJ/t_{PP+PE}). Therefore, given the low-temperature heat needed for DAC, plant-level integration of heat is key: 22% heat saving is enabled by the HI-plant integration with state-of-the-art DAC, which increases to 48% heat saving when DAC includes more advanced technologies (primarily sorbent and contactor development). The direct heat consumption of the PL route is significantly smaller than that of the DAC route, positioning at around 2.85−11.00 GJ/t_{PP+PE}. Also in this case, heat integration at the plant level is important, as it significantly lowers the total direct heat consumption (specifically for the separations in the syngas-to-methanol process). It is also worth stressing that plant-level heat integration removes the need for a high-temperature heat supply in the CCU pathway, thereby eliminating the H_2 input. Moreover, the plant-level integration makes the BMG route heat-neutral while largely reducing the heat consumption in the ETOH route from 4.65 to 1.07 GJ/t_{PP+PE}.

To conclude, the BIO pathway requires much less direct heat and electricity than the CCU pathway and fossil PE and PP (an average of 17.85 GJ/t_{PP+PE} from naphtha cracking and polymerization).[52] The net direct electricity balance of the CCU routes is not particularly affected by technology development, neither for DAC nor for PL routes. On the contrary, the direct heat requirement is significantly reduced by plant-level heat integration and technology development, which often provides synergistic effects (e.g., lower temperatures for sorption-enhanced RWGS favor heat integration). The net direct electricity balance of the BMG and ETOH routes depends on technology development, while the net direct heat balance is primarily driven by plant-level heat integration.

Overall Energy Input and Energy Efficiency

Figure 6 shows the total energy input, including hydrogen and biomass, and the system energy efficiency. For the sake of clarity, the total energy input has been normalized, thereby showing the respective contribution of the direct electricity input vs the embedded energy in hydrogen and biomass. While the production of fossil-free PE and PP has lower energy consumption than fossil PE and PP when considering only the electricity input to the fossil-free plant—with the exception of the DAC−CCU route—the balance shifts abruptly when accounting for the energy content in the hydrogen and biomass feedstock. The electricity input to the plant accounts for around 5 to 15% of the total energy provided to the full system. This poses a critical challenge for the supply (i) of green electricity in H_2 electrolyzers or (ii) of sustainable biomass.

As for the overall energy efficiency, which is shown on the secondary *y*-axis of Figure 6, it can be noted that the values are in a similar range for all routes. More specifically, the DAC route with standard technology and process-level heat integration has the lowest energy efficiency at 26%, increasing to 29% when more advanced technologies and plant-level heat integration are considered. The other three routes have around 30% energy efficiency, increasing slightly with technology development and heat integration. The key reason for the energy efficiency remaining roughly constant is the minor contribution of the process energy consumption compared to the energy input supplied by the material feedstock. This result indicates that energy efficiency can be effectively enhanced only by increasing H_2 electrolysis efficiency in the CCU

https://doi.org/10.1021/acsomega.5c09670
ACS Omega 2026, 11, 4314−4332

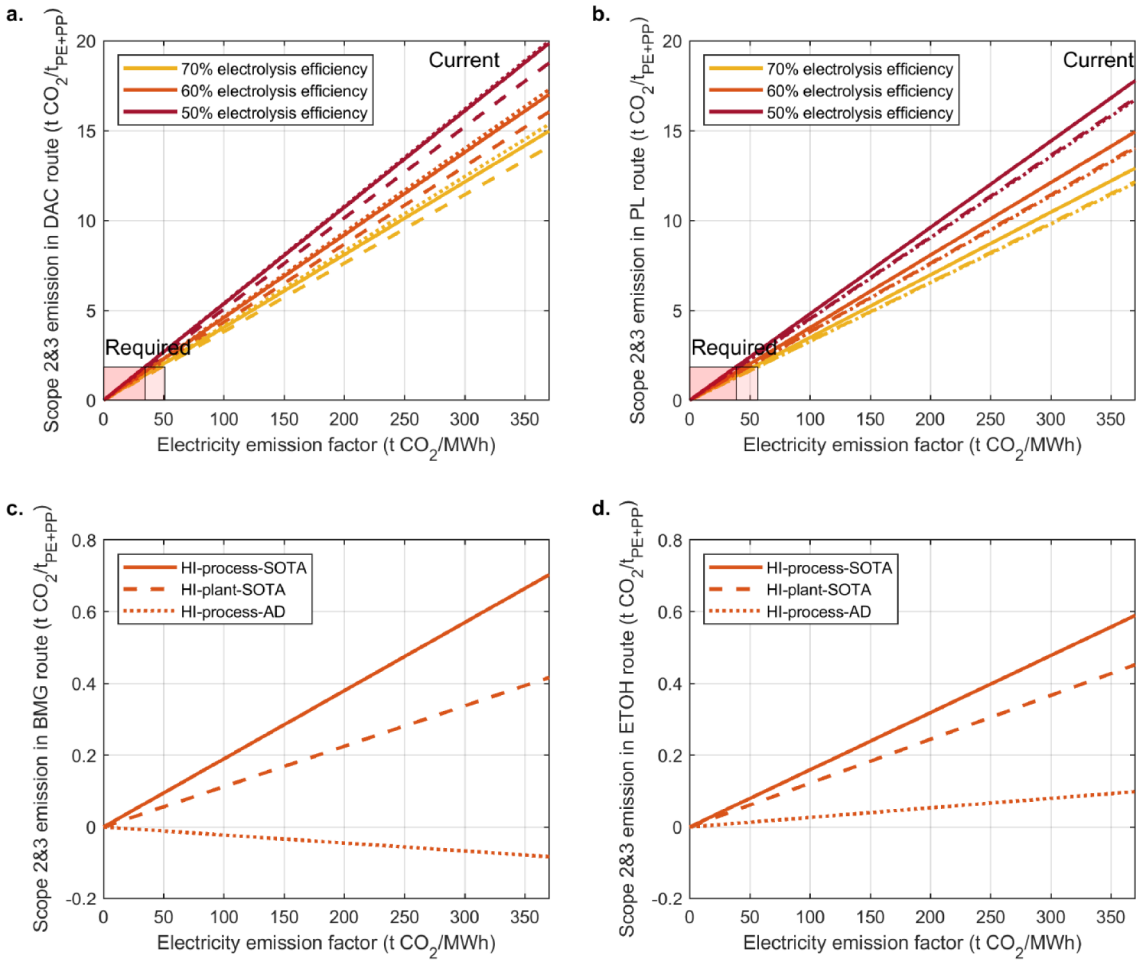

Figure 7. CO_2 missions vs electricity emission factor and H_2 electrolysis efficiency in the assessed for the 12 different cases considered in the paper (DAC, PL, BMG, ETOH for HI-process-SOTA/HI-plant-SOTA/HI-pant-AD): yellow, orange, and red colors show H_2 electrolysis efficiency from 70% to 50%; solid and dashed lines show HI-process-SOTA, HI-plant-SOTA and HI-plant-AD cases; the red area shows the required electricity emission factor to ensure lower emissions of fossil-free PE and PP than fossil PE and PP.

pathway and biomass harvesting in the BIO pathway. It is also worth noting that the energy efficiency of fossil-free pathways is only half that of the fossil-derived pathway (50%−60%) owing to the different processes in the different pathways.[53]

Emissions

In designing the different routes, we consider providing—whenever needed—low-temperature heat by heat pumps and high-temperature heat by H_2 boilers, thereby leaving electricity, biomass, and hydrogen itself as the only energy sources. Given that we consider sustainable biomass as feedstock (accounting for the life cycle emissions of biomass is amply done in the literature and beyond the scope of this work), the CO_2 emissions of the four routes only come from electricity consumption directly involved in the process and for H_2 production. Figure 7 shows how the emissions vary with the electricity emission factor and H_2 electrolysis efficiency. The DAC and PL routes have high electricity consumption owing to H_2 electrolysis, thus requiring the electricity emission factor to be significantly lower than the current one to result in lower emissions than those of fossil PE and PP (1.85 t CO_2/t for landfill, HDPE, EASEWASTE database).[54,55] More specifically, if H_2 electrolysis efficiency is only 50%, the electricity emission factor would need to be around 30 t of CO_2/MWh. On the other hand, the BIO pathway has much lower electricity consumption, leading to CO_2 emissions significantly lower than those of fossil PE and PP, even with the current electricity emission factor. It should be noted that direct emissions at the plant level (excluding H_2 production) are lower for all routes compared to fossil PE and PP (see Figures 2 - 5 in the SI). This might open interesting opportunities for producers, who will most likely import H_2 rather than produce it on-site, depending on the carbon crediting market.

Carbon Efficiency

Figures 8−10 show the carbon efficiency, which accounts for how many carbon molecules from the feedstock end up in the final product. For simplification, the carbon efficiency is reported exclusively for the SOTA scenario. Moreover, it is worth noting that internal recycling of CO_2, for example, with carbon capture from process emissions, is not considered here (as it is outside the scope of this study). Results show that the DAC and PL routes in the CCU pathway have similar carbon efficiency: 83% of carbon from feedstock ends up in primary (64%) and secondary products (19%), which are mostly produced in the MTO process. The remaining 17% ends up in CO_2 from the combustion of residuals (9%) and in high LHV hydrocarbon streams with little or close-to-zero market value (8%). Further catalyst improvements and better/more separation steps can increase the carbon efficiency further;

https://doi.org/10.1021/acsomega.5c09670
ACS Omega 2026, 11, 4314−4332

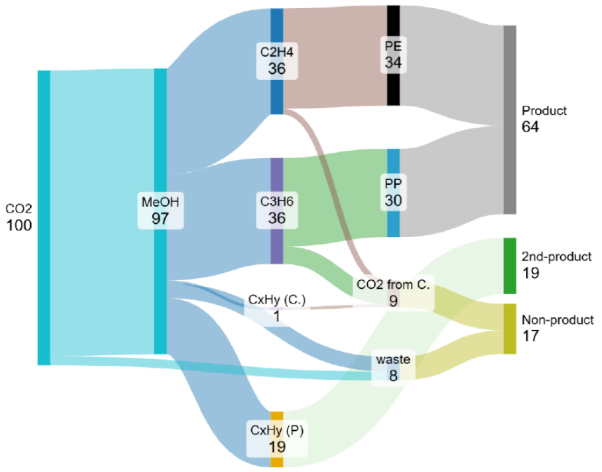

Figure 8. Carbon flow in the CCU pathway in the SOTA scenario: CxHy (P) indicates valuable secondary product flow in the MTO process; CxHy (C.) indicates high-LHV streams from the MTO process for combustion; and CO_2 from C. indicates the CO_2 from residual fuel gas combustion.

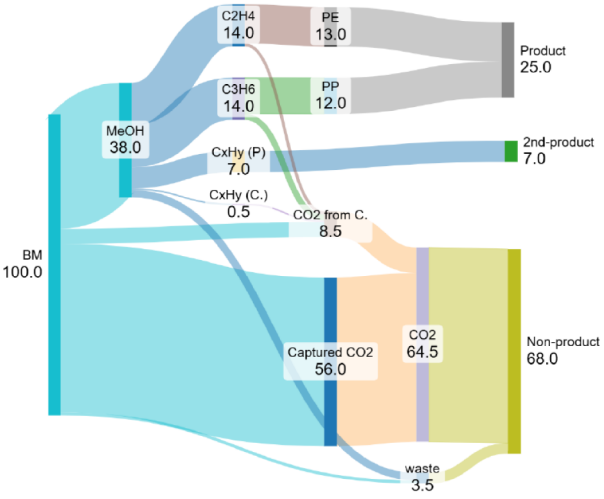

Figure 9. Carbon flow in the BIO-BMG route in the SOTA scenario: CxHy (P) indicates valuable secondary product flow in the MTO process; CxHy (C.) indicates high-LHV streams from the MTO process for combustion; CO_2 from C. indicates the CO_2 from residual fuel gas combustion.

however, these may not be economically optimal, as residual combustion replaces expensive hydrogen imports.

Looking at the BIO pathway, the carbon efficiency is significantly lower than the CCU pathway: in the BMG route, 32% of carbon ends up in primary (25%) and secondary (7%) products, while in the ETOH route, 26% of carbon ends up in the primary product (no secondary products are present in the ETOH route). In the BMG route, 56% of carbon is lost in the form of CO_2 in the gasification island, where carbon is combusted in the reactor to provide heat and maintain the temperature at 870−920 °C. The secondary products are once again produced in the MTO process, similarly to the CCU case. In the ETOH route, ETOH fermentation can only utilize cellulose and hemicellulose at maximum 67% carbon efficiency according to the chemical reaction stoichiometry. Additionally, a large amount of carbon exists in lignin, acid, and other unusable compositions (33%) that cannot be fermented and

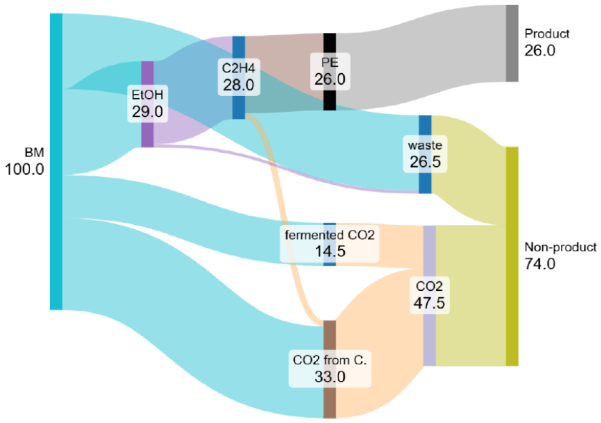

Figure 10. Carbon flow in the BIO-ETOH route in the SOTA scenario: CO_2 from C. indicates the CO_2 from residual fuel gas combustion.

are combusted for heat recovery. As a result, only 29% of carbon from wood pellets is converted into ETOH and further transformed into PE (26%). Compared to the carbon efficiency of fossil-derived PE&PP (ca. 52%), the CCU pathway shows higher carbon efficiency, while BIO pathways result in lower carbon efficiency.[56]

Economic Assessment

Figure 11 shows the levelized specific cost of PE and PP (EUR/t_{PP+PE}). The DAC route is consistently the most expensive among the four assessed routes, producing PE and PP at 5,348 EUR/t_{PP+PE} in the HI-process-SOTA case. As shown by the breakdown per process, the high cost is associated with (i) OPEX and CAPEX of capturing CO_2 from the air and (ii) the purchase of H_2 as a CO_2 reducing agent and feedstock. While plant-level heat integration has limited effects on costs, mostly associated with a reduction in the import of H_2, technological advancements contribute more effectively: cheaper and more efficient DAC reduces the total cost by around 15%. It was found, however, that the cost decrease associated with the adoption of sorption-enhanced RWGS is limited, mostly due to the minor contribution of the RWGS to the energy input and overall costs. In all scenarios, we can conclude that the DAC route struggles to be economically competitive with other fossil-free PE and PP, let alone fossil-based PE and PP.

Moving to the PL route, the levelized specific cost decreases to 4,200 EUR/t_{PP+PE} in the HI-process-SOTA case, cheaper than the DAC route but is almost double that of the two biomass routes. By implementing plant-level heat integration and advanced technology, the cost is expected to decline by 4% and 5%. It is worth stressing that sourcing CO_2 has a non-negligible contribution to the total costs.

The BMG route is the second cheapest among the four routes, approaching 2,690 EUR/t_{PP+PE} in the HI-process-SOTA case. Furthermore, the deployment of plant-level heat integration has a minor effect, reducing the cost by 2%; technology advancement plays a more significant role, as the cost can be decreased by 18% by advancing pressurized biomass gasification, which removes the expensive compression.

Finally, the ETOH route has the lowest cost, approaching 2,144 EUR/t_{PP+PE} in the HI-process-SOTA case. Notably, the production cost can be reduced by plant-level heat integration

https://doi.org/10.1021/acsomega.5c09670
ACS Omega 2026, 11, 4314−4332

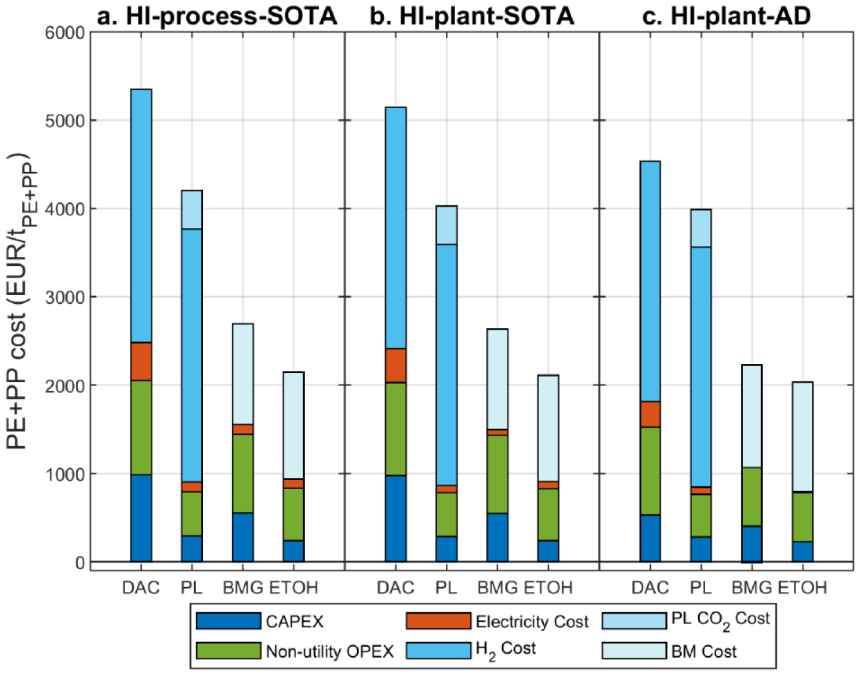

Figure 11. Levelized cost of PE+PP for the 12 different cases considered in the paper (DAC, PL, BMG, ETOH for HI-process-SOTA/HI-plant-SOTA/HI-pant-AD). The cost is broken down into different categories (CAPEX, utility cost, material cost and other OPEX) and color-coded as shown in the legend.

and ETOH reaction integration by only 1% and 5%, respectively. The low cost of the ETOH route and the modest improvement by advanced technologies are expected, as the entire process of the ETOH route has already been commercialized. It is worth stressing that the ETOH route can only produce PE instead of coproducing PE and PP.

The Effect of Feedstock and Energy Price. For all of the routes, the electricity cost accounts for less than 7% of the total cost. Over 40% of the total cost is consistently attributed to the material cost (H_2, CO_2 and wood pellets); the material cost proportion to the total cost peaks for the PL route in HI-process-SOTA at 77%. In the CCU pathway, H_2 consumption differs depending on heat integration and technology level—the more integrated and advanced case consumes slightly less H_2 owing to lower high-temperature heat demand and reduced reducing agent demand—but the DAC route and PL route have substantially similar H_2 consumption. In the BIO pathway, biomass consumption per tonne of PE and PP varies subtly with scenarios and heat integration levels, yet more obviously with different routes because of the higher carbon efficiency toward products and secondary products in the BMG route. In other words, in all cases, material cost dominates; yet their market prices are highly uncertain: the market for green H_2 and CO_2 does not exist, and the price of wood pellets is highly dependent on production location and transportation. Therefore, we reassess all different cases by varying the price of the key feedstock: H_2 for the CCU pathway and biomass pellets for the BIO.

Figure 12 shows the levelized cost of PE+PP for varying hydrogen prices (roughly between 1 and 6 EUR/kgH_2). As expected, small changes in hydrogen prices lead to major cost fluctuations in the product costs. The product cost for the DAC scenario remains high over the entire range of hydrogen costs, varying between 3,000 and 6,000 EUR/t_{PP+PE}. The product cost for the CCU scenario is significantly lower, but

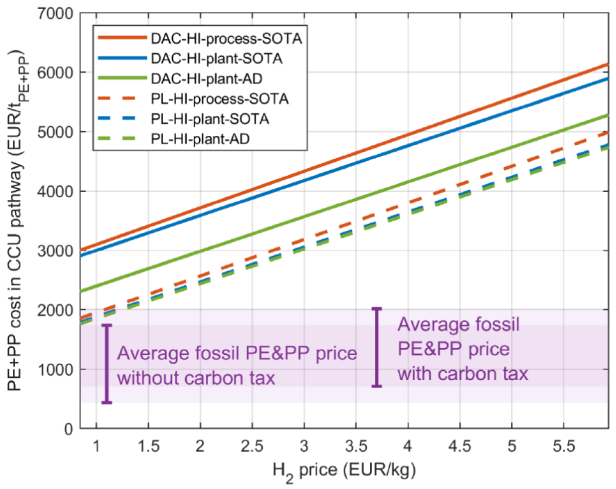

Figure 12. Levelized PE and PP cost in the CCU pathway vs H_2 price in three cases (SOTA/HI-plant-SOTA/HI-pant-AD). Solid lines indicate the DAC route and the dashed lines indicate the PL route; the three colors indicate three cases; the purple area indicates the fossil PE and PP price range from 2014 to 2022, fluctuating with carbon tax (150 EUR/t CO_2).[57,58]

the variation is in line with the DAC case: between 2,000 and 5,000 EUR/t_{PP+PE}. All CCU cases remain substantially more expensive than fossil PE and PP without a carbon tax, even when considering historical averages (1,000−1,500 EUR/t during 2014−2022).[57,58] This should not come as a surprise: fossil fuels are and remain the cheapest way to produce chemicals when their detrimental effects on the environment are not accounted for. When considering a carbon tax of 150 EUR/t CO_2 and emissions of 1.85 kg/kg_{PP+PE},[54,55] the pipeline CCU case becomes cheaper than the fossil price of PE and PP for very small hydrogen prices, at around 1.2 EUR/kg. However, this is still higher than the current cost of hydrogen

https://doi.org/10.1021/acsomega.5c09670
ACS Omega 2026, 11, 4314−4332

produced from natural gas. Therefore, adequately accounting for the CO_2 emissions during the lifetime of PE and PP (i.e., including the end of life) is a required condition to produce fossil-free PE and PP via CCU.

Figure 13 shows the levelized cost of PE+PP for varying biomass prices (between 80 and 240 EUR/$t_{Biomass}$). It can be noted that the biomass price has a significant effect on the PE and PP cost, yet it is limited compared to the hydrogen price in the CCU route. Biobased PP and PE have a resulting cost that varies between 1,500 and 3,250 EUR/t_{PP+PE}. Moreover, the effect of the feedstock price affects all biobased routes similarly. Interestingly, the cost of biobased PE and PP becomes competitive with the fossil counterpart over a moderate range of prices, even in the absence of subsidies or CO_2 emissions pricing. Accounting for a carbon tax at 150 EUR/t CO_2), biobased PE−PP are cost-comparable with fossil-derived PP−PE, even at the current price of wood pellets. It is therefore expected that, when economically accounting for the harm caused by fossil-derived PE−PP and under the hypothesis of sustainable biomass availability, biobased PE−PP will become a preferred manufacturing route.

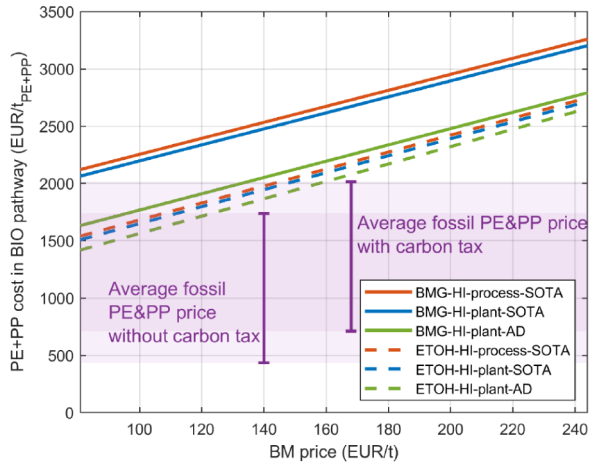

Figure 13. Levelized PE and PP cost in the BIO pathway vs wood pellet price in three cases (SOTA/HI-plant-SOTA/HI-pant-AD). Solid lines indicate the BMG route and the dashed lines indicate the ETOH route; the three colors indicate three cases; the purple area indicates the fossil PE and PP price range from 2014 to 2022, fluctuating with carbon tax (150 EUR/t CO_2).[57,58]

Summary of Results and Routes Comparison

All KPIs of the four routes are summarized in Table 6. By comparing them, we can draw the following conclusions.

- The energy efficiency of the four routes is similar, reaching values around 30%. The DAC and PL routes in the CCU pathway perform at high carbon efficiency, however the high energy consumption of CCU is demanding in terms of accessing green electricity to achieve low emissions. Our results show that electricity needs to have an emission factor of at least 1/7 of the current emission factor to make CCU pathway a CO_2 mitigation process.
- In comparison, the BIO pathway can only convert approximately 25% carbon into PE and PP, with no trivial advanced technology in sight for substantial improvement in the carbon efficiency. While a substantial amount of carbon is lost in biomass conversion, the carbon loss can be used in energy production processes. As a promising alternative option, the carbon loss could be fed to the CCU pathway, obtaining a potential significant synergy between the BIO and CCU pathways.
- The cost of fossil-free PE and PP is primarily driven by the feedstock price, hydrogen for CCU and biomass pellets for BIO. The CCU pathway is particularly expensive, and the key to lowering the cost is accessing cheap H_2, along with enhanced efficiency obtained from plant-level heat integration and more advanced technologies. The BIO pathway is significantly cheaper than the CCU pathway but is still at least one-and-a-half times of the average price of fossil PE and PP, becoming cheaper when the wood pellets cost less than 132 EUR/t.

Table 6. Result Summary of KPIs

Route	KIP	HI-process-SOTA	HI-plant-SOTA	HI-plant-AD
CCU-DAC[a]	Cost (EUR/t_{PP+PE})	5,348	5,144	4,531
	Electricity consumption (GJ/t_{PP+PE})	27.02	24.05	18.21
	Feedstock (H_2) (t/t_{PP+PE})	0.71	0.67	0.67
	Energy efficiency	26%	28%	29%
	Carbon efficiency	64%	64%	64%
	Emission (tCO_2/t_{PP+PE})	-	-	-
CCU-PL[b]	Cost (EUR/t_{PP+PE})	4,200	4,026	3,986
	Electricity consumption (GJ/t_{PP+PE})	6.83	5.03	5.07
	Feedstock (H_2) (t/t_{PP+PE})	0.71	0.67	0.67
	Feedstock (CO_2) (t/t_{PP+PE})	4.96	4.96	4.87
	Energy efficiency	30%	31%	32%
	Carbon efficiency	64%	64%	64%
	Emission (tCO_2/t_{PP+PE})	0.70	0.52	0.52
BIO-BMG	Cost (EUR/t_{PP+PE})	2,690	2,633	2,212
	Electricity consumption (GJ/t_{PP+PE})	6.84	4.05	−0.80
	Feedstock (biomass) (t/t_{PP+PE})	8.04	8.04	8.16
	Energy efficiency	31%	31%	32%
	Carbon efficiency	25%	25%	25%
	Emission (tCO_2/t_{PP+PE})	0.70	0.42	-[c]
BIO-ETOH	Cost (EUR/t_{PP+PE})	2,144	2,112	2,036
	Electricity consumption (GJ/t_{PP+PE})	5.74	4.40	0.96
	Feedstock (biomass) (t/t_{PP+PE})	7.43	7.43	7.61
	Energy efficiency	32%	32%	32%
	Carbon efficiency	26%	25%	25%
	Emission (t_{PP+PE}/t_{PP+PE})	0.56	0.45	0.10

[a]It is assumed DAC route is only available when electricity is green for both H_2 electrolysis and grid, and the current emission factor is not applicable to the KPI assessment of DAC route. [b]The current emission factor is used for process electricity on the KPI assessment of PL route. [c]BMG route in HI-plant-AD case exports electricity and the emission factor is not applicable.

https://doi.org/10.1021/acsomega.5c09670
ACS Omega 2026, 11, 4314−4332

DISCUSSION

Four fossil-free PE and PP production routes—direct air capture (DAC), pipeline CO_2 (PL), biomass gasification (BMG), and ethanol fermentation (ETOH)—were designed and evaluated across three scenarios using a harmonized modeling framework incorporating process models and techno-economic assessment (TEA) modules. The three scenarios include: (i) process-level heat integration under state-of-the-art conditions (HI-process-SOTA), (ii) plant-level heat integration under state-of-the-art conditions (HI-plant-SOTA), and (iii) plant-level heat integration with advanced technologies (HI-plant-AD). The assessment considered energy consumption, energy efficiency, carbon efficiency, emissions, and cost, as summarized in Table 6.

The different results for each route in the three scenarios indicate an effective strategy to improve state-of-the-art fossil-free PE and PP manufacturing. All of the routes substantially benefit from cross-process heat integration, leading to reduced electricity consumption combined with heat pumps. This strategy requires that all the subplants be built on one site, which might not be realized because of the lack of land and infrastructure. Technological breakthroughs in CO_2 mining and fossil-free carbon feedstock conversion are also important in enhancing the competitiveness of fossil-free PE and PP production. The DAC route can focus on scale-up and sorbent development to mine CO_2 from air; the improvement of the BMG route requires the development of a pressurized gasification system; the ETOH route might see slight improvement by implementing steam explosion pretreatment and integrating fermentation reactors. Again, some of the considered technological breakthroughs might be optimistic, especially in large-scale applications.

Comparisons with the existing literature highlight some deviations. For instance, the carbon efficiency of the BMG process in this study is 34%, approximately 8% points lower than that reported by Poluzzi et al., due to differences in gasifier performance data.[48] The energy efficiency in the ETOH process (32%) is also lower than that reported by Hamelinck et al. (by 6% points), again attributable to differing yield data.[59] Zhao et al. reported significantly lower costs for BMG and ETOH routes in China (below 820 EUR/t olefins), largely due to substantially lower biomass prices.[1] On the other hand, our results for the DAC route are highly similar to those from Allgoewer et al.[12]—in terms of electricity consumption (5% difference), heat consumption (47% difference due to the STM process, though other processes have similar results), and cost (25% difference).

The high costs and energy demands identified in this study underscore the importance of low-cost inputs, advanced technologies, and plant-level heat integration in making fossil-free PE and PP viable. Above all, it shows that benchmarking these new PE−PP production routes with fossil fuels PE and PP is not, and will likely never be, fair: the cost of pollution and climate damage from fossil fuel consumption must be embedded in fossil-based chemicals. When green electricity is available, selecting the optimal route between the ETOH route, PL route, and DAC route depends on material availability. BMG is less attractive when suitable biomass is available for ethanol fermentation, as the ETOH route generally offers superior KPIs. However, if the available biomass has low hemicellulose and cellulose composition, the ETOH route may lead to low conversion, and the BMG route might become preferable thanks to its flexibility with respect to feedstock quality.

The assessment assumes that all of the involved technologies are scalable. However, scaling up is challenging for some technologies. DAC is still in its infancy, and manufacturing capacity will be limited in the short term. The RWGS reaction—operated at a high temperature in the gas phase—may necessitate parallel reactor trains at large scales. The BMG route faces challenges in continuous operation and in sourcing sufficient biomass locally, limiting both operational and logistical scalability. Similar constraints apply to the ETOH process, where the plant size is limited by local biomass availability. Moreover, the reliance on lab- or pilot-scale data introduces uncertainty in extrapolating to industrial-scale performance, particularly with respect to reaction conversions.

Despite efforts to ensure robust modeling, significant uncertainties remain—especially concerning costs. Hydrogen and biomass together contribute more than 40% of the total production costs, yet their prices are highly uncertain. The hydrogen market remains underdeveloped, and biomass prices are heavily influenced by logistics. Reactor CAPEX also represents a major source of uncertainty; due to the need for bespoke reactor designs, standard cost correlations are insufficient. More detailed reactor engineering and validation by engineering, procurement, and construction (EPC) firms would improve the reliability of capital cost estimates.

CONCLUSIONS

Our study designed and assessed four defossilized production routes for polyethylene and polypropylene (PE and PP) using fossil-free carbon sources and renewable energy. The routes include: (i) CCU via direct air capture (DAC) of CO_2 reduced with H_2, (ii) CCU via pipeline-transported CO_2 reduced with H_2 (PL route), (iii) biobased with woody biomass gasification (BMG route), and (iv) biobased with ethanol fermentation from woody biomass (ETOH route). All routes were process-designed and techno-economically assessed within a harmonized modeling framework developed in ASPEN Plus and MATLAB to ensure comparability. The analysis covers the full value chain from feedstocks to final PE and PP products.

The results indicate that the optimal route depends on the specific performance metric under consideration: cost, energy efficiency, or carbon efficiency. The ETOH route is the most cost-effective at 2,036 EUR/t_{PP+PE}, the BMG route is the most energy-efficient at 32%, while the two CCU routes (DAC and PL) exhibit the highest carbon efficiency—64%, or up to 83% when including secondary products.

Despite the environmental advantages of fossil-free PE and PP, their economic viability remains uncertain. Currently, the cost of fossil-free PE and PP is two to four times higher than the average price of fossil PE and PP.[57,58] However, reducing the price of wood pellets to 81 EUR/t could lower the cost of the BIO pathway to 1,433 EUR/t_{PP+PE}, and a hydrogen price of 0.8 EUR/kg could reduce the CCU pathway cost to 1,762 EUR/t_{PP+PE}. Furthermore, fossil PE and PP prices are highly volatile and, in 2021, exceeded those of fossil-free alternatives (1,579−1,996 EUR/t). It remains, however, imperative to consider the detrimental effects of fossil fuels on climate and ecosystems: introducing a fair carbon taxation would increase the cost of fossil-derived PE and PP while making fossil-free alternatives more attractive.

The BIO pathway requires substantial biomass input, while the CCU routes demand significant amounts of green

https://doi.org/10.1021/acsomega.5c09670
ACS Omega 2026, 11, 4314−4332

electricity to match current PE and PP production levels—thus highlighting the challenges for the supply of renewable electricity and sustainable biomass. Future improvements in key performance indicators (KPIs) rely on enhancing H_2 electrolysis efficiency, using pressurized biomass gasifiers, increasing biomass conversion yields, and implementing plant-level heat integration.

While the primary aim of this work is to provide a harmonized assessment, some limitations remain. Reactor CAPEX data were derived from heterogeneous sources with inconsistent design and costing standards, precluding full harmonization. Additionally, the large number of processes that were designed in Aspen Plus required limiting the level of detail; this leaves ample opportunities for improving the thermodynamic description, for example, through refined kinetic modeling and recycle loop design. Moreover, mathematical optimization of the different processes could further improve the performance of the plants by unlocking nontrivial, nonstandard configurations.

This study not only compares the KPIs of four representative fossil-free PE and PP manufacturing routes but also delivers a modeling framework that can be modified to suit different economic scenarios and test different heat integration strategies. Open-sourced cost databases and process models of fossil-free processes can also be integrated into this modeling framework to include more fossil-free routes, thereby further driving the net-zero transition.

■ ASSOCIATED CONTENT

Supporting Information

The Supporting Information is available free of charge at https://pubs.acs.org/doi/10.1021/acsomega.5c09670.

Supplementary results and detailed process design descriptions (PDF)

■ AUTHOR INFORMATION

Corresponding Author

Matteo Gazzani − *Copernicus Institute of Sustainable Development, Utrecht University, Utrecht 3584 CB, The Netherlands;* orcid.org/0000-0002-1352-4562; Email: m.gazzani@uu.nl

Authors

Shiyu Ding − *Copernicus Institute of Sustainable Development, Utrecht University, Utrecht 3584 CB, The Netherlands*

Gert Jan Kramer − *Copernicus Institute of Sustainable Development, Utrecht University, Utrecht 3584 CB, The Netherlands*

André Faaij − *TNO, Amsterdam 1043 NT, The Netherlands; Copernicus Institute of Sustainable Development, Utrecht University, Utrecht 3584 CB, The Netherlands*

Juliana Garcia Moretz-Sohn Monteiro − *TNO, Amsterdam 1043 NT, The Netherlands;* orcid.org/0000-0002-2954-2466

Complete contact information is available at: https://pubs.acs.org/10.1021/acsomega.5c09670

Notes

During the preparation of this work, the authors used ChatGPT to improve language and readability. After using this tool, the authors reviewed and edited the content as needed and took full responsibility for the content of the publication.

The authors declare no competing financial interest.

■ ACKNOWLEDGMENTS

This work was supported by the Industrial Transformation programme of The Netherlands Organisation for Applied Scientific Research (TNO). Authors thank Ric Hoefnagels from Utrecht University and Berend Vreugdenhil from TNO for discussing and supporting the analysis of the biomass pathway.

■ ADDITIONAL NOTE

[1]We acknowledge that CO_2 from pipeline cannot be considered as CO_2-neutral carbon—likely it will derive from fossil fuel carbon capture; however, given the variety of possible sources and the fact that it goes beyond the paper scope, we prefer to simplify the analysis of the pipeline route and keep it in line with DAC- or biomass-sourced carbon.

■ REFERENCES

(1) Zhao, Z.; Jiang, J.; Wang, F. An economic analysis of twenty light olefin production pathways. *J. Energy Chem.* **2021**, *56*, 193−202.

(2) Zühlsdorf, B.; Bühler, F.; Bantle, M.; Elmegaard, B. Analysis of technologies and potentials for heat pump-based process heat supply above 150 °C. *Energy Convers. Manage.* **2019**, *2*, 100011.

(3) Ferdous, J.; Bensebaa, F.; Pelletier, N. Integration of LCA, TEA, process simulation and optimization: A systematic review of current practices and scope to propose a framework for Pulse Processing Pathways. *J. Cleaner Prod.* **2023**, *402*, 136804.

(4) Kang, C.; Liu, J. J.; Woo, N.; Won, W. Process Design for the Sustainable Production of Butyric Acid Using Techno-Economic Analysis and Life Cycle Assessment. *ACS Sustainable Chem. Eng.* **2023**, *11*, 4430−4440.

(5) Rubin, E. S.; Davison, J. E.; Herzog, H. J. The Cost of CO2 Capture and Storage. *Int. J. Greenhouse Gas Control* **2015**, *40*, 378−400.

(6) van der Spek, M.; Bonalumi, D.; Manzolini, G.; Ramirez, A.; Faaij, A. Techno-economic comparison of combined cycle gas turbines with advanced membrane configuration and monoethanol-amine solvent at part load conditions. *Energy Fuels* **2018**, *32*, 625−645.

(7) Poluzzi, A.; Guandalini, G.; Romano, M. C. Flexible Methanol and Hydrogen Production from Biomass Gasification with Negative Emissions. *Sustainable Energy Fuels* **2022**, *6* (16), 3830−3851.

(8) Anicic, B.; Trop, P.; Goricanec, D. Comparison between two methods of methanol production from carbon dioxide. *Energy* **2014**, *77*, 279−289.

(9) Ortiz-Espinoza, A. P.; Noureldin, M. M. B.; El-Halwagi, M. M.; Jiménez-Gutiérrez, A. Design, simulation and techno-economic analysis of two processes for the conversion of shale gas to ethylene. *Comput. Chem. Eng.* **2017**, *107*, 237−246.

(10) Voldsund, M.; Gardarsdottir, S. O.; De Lena, E.; Pérez-Calvo, J.-F.; Jamali, A.; Berstad, D.; Fu, C.; Romano, M.; Roussanaly, S.; Anantharaman, R.; et al. Comparison of technologies for CO2 capture from cement production—part 1: Technical evaluation. *Energies* **2019**, *12* (3), 559.

(11) Gardarsdottir, S. O.; De Lena, E.; Romano, M.; Roussanaly, S.; Voldsund, M.; Pérez-Calvo, J.-F.; Berstad, D.; Fu, C.; Anantharaman, R.; Sutter, D.; et al. Comparison of technologies for CO2 capture from cement production—part 2: Cost analysis. *Energies* **2019**, *12* (3), 542.

(12) Allgoewer, L.; Becattini, V.; Patt, A.; Grandjean, P.; Wiegner, J. F.; Gazzani, M.; Moretti, C. Cost-Effective Locations for Producing Fuels and Chemicals from Carbon Dioxide and Low-Carbon Hydrogen in the Future. *Ind. Eng. Chem. Res.* **2024**, *63*, 13660−13676.

(13) Zhao, X.; You, F. Consequential life cycle assessment and optimization of high-density polyethylene plastic waste chemical recycling. *ACS Sustainable Chem. Eng.* **2021**, *9*, 12167−12184.
(14) Cappello, V.; Sun, P.; Zang, G.; Kumar, S.; Hackler, R.; Delgado, H. E.; Elgowainy, A.; Delferro, M.; Krause, T. Conversion of plastic waste into high-value lubricants: Techno-Economic Analysis and Life Cycle Assessment. *Green Chem.* **2022**, *24* (16), 6306−6318.
(15) Trucillo, P.; Rizzo, M.; Errico, D.; Di Maio, E. Social, economic, and environmental impacts of bio-based versus Fossil-derived polyethylene production. *Adv. Sustainable Syst.* **2025**, *9* (1), 2400392.
(16) Uekert, T.; Singh, A.; DesVeaux, J. S.; Ghosh, T.; Bhatt, A.; Yadav, G.; Afzal, S.; Walzberg, J.; Knauer, K. M.; Nicholson, S. R.; Beckham, G. T.; Carpenter, A. C. Technical, economic, and environmental comparison of closed-loop recycling technologies for common plastics. *ACS Sustainable Chem. Eng.* **2023**, *11*, 965−978.
(17) Hernández, B.; Kots, P.; Selvam, E.; Vlachos, D. G.; Ierapetritou, M. G. Techno-economic and life cycle analyses of thermochemical upcycling technologies of low-density polyethylene waste. *ACS Sustainable Chem. Eng.* **2023**, *11*, 7170−7181.
(18) International Energy Agency. *The Future of Petrochemicals—Towards a more sustainable chemical industry*; International Energy Agency, 2018.
(19) McQueen, N.; Gomes, K. V.; McCormick, C.; Blumanthal, K.; Pisciotta, M.; Wilcox, J. A Review of Direct Air Capture (DAC): Scaling up Commercial Technologies and Innovating for the Future. *Prog. Energy* **2021**, *3*, 032001.
(20) Sabatino, F.; Grimm, A.; Gallucci, F.; van Sint Annaland, M.; Kramer, G. J.; Gazzani, M. A Comparative Energy and Costs Assessment and Optimization for Direct Air Capture Technologies. *Joule* **2021**, *5*, 2047−2076.
(21) Valentine, J.; Zoelle, A.; Homsy, S.; Mantripragada, H.; Woods, M.; Roy, N.; Kilstofte, A.; Sturdivan, M.; Steutermann, M.; Fout, T. *Direct Air Capture Case Studies: Sorbent System*; National Energy Technology Laboratory (NETL), 2022.
(22) Baylin-Stern, A.; Beck, L. *Direct Air Capture A Key Technology For Net Zero*; OECD, 2021.
(23) Brownsort, P. A. *Carbon Dioxide Pipelines: A Preliminary Review*; 2024.
(24) Verdegaal, W. M.; Becker, S.; von Olshausen, C. Power-to-Liquids: Synthetisches Rohöl aus CO2, Wasser und Sonne. *Chem. Ing. Tech.* **2015**, *87* (4), 340−346.
(25) Pieterse, J. A. Z.; Elzinga, G. D.; Booneveld, S.; van Kampen, J.; Boon, J. Reactive Water Sorbents for the Sorption-Enhanced Reverse Water−Gas Shift. *Catal. Lett.* **2022**, *152*, 460−466.
(26) Ott, J.; Gronemann, V.; Pontzen, F.; Fiedler, E.; Grossmann, G.; Kersebohm, D. B.; Weiss, G.; Witte, C. Methanol. In *Ullmann's encyclopedia of industrial chemistry*; Wiley, 2000.
(27) Tian, P.; Wei, Y.; Ye, M.; Liu, Z. Methanol to olefins (MTO): From fundamentals to commercialization. *ACS Catal.* **2015**, *5*, 1922−1938.
(28) Chen, Y.-H.; Hsieh, W.; Chang, H.; Ho, C.-D. Design and economic analysis of industrial-scale methanol-to-olefins plants. *J. Taiwan Inst. Chem. Eng.* **2022**, *130*, 103893.
(29) Almansa, G. A.; Vilela, C. M.; Vreugdenhil, B. *Gas analysis in gasification of biomass and waste - IEA bioenergy*; 2018, https://www.ieabioenergy.com/wp-content/uploads/2018/09/IEA-Bioenergy-Task-33-gas-analysis-report-Document-1-1.pdf.
(30) Voima, V.*Vaasa Bio-Gasification Power Plant*2013https://www.renewable-technology.com/projects/vaasa-bio-gasification-power-plant/ Accessed: 02 February 2024
(31) Jafri, Y.; Waldheim, L.; Lundgren, J. *Emerging Gasification Technologies For Waste & Biomass*; IEA Bioenergy, 2020.
(32) Sikarwar, V. S.; Zhao, M.; Clough, P.; Yao, J.; Zhong, X.; Memon, M. Z.; Shah, N. J. E.; Anthony; Fennell, P. S. An overview of advances in biomass gasification. *Energy Environ. Sci.* **2016**, *9*, 2939−2977.
(33) Hamelinck, C. N.; Faaij, A. P. C. Future prospects for production of methanol and hydrogen from biomass. *J. Power Sources* **2002**, *111*, 1−22.
(34) Mia, R.; Seifert, H.; Haag, W.; Leibold, H.; Heidenreich, S. Operating Behaviour of a Multi-Candle Filter with Coupled Pressure Pulse Re-cleaning during Normal Operation and in the Case of Filter Candle Failure. In *Proceedings Of 5th International Symposium On Gas Cleaning At High Temperature*; Fraunhofer Verlag, 2002.
(35) Cormos, C.-C. Green Hydrogen Production from Decarbonized Biomass Gasification: An Integrated Techno-Economic and Environmental Analysis. *Energy* **2023**, *270*, 126926.
(36) *Flagship (first-of-a-kind commercial) and demonstration cellulosic ethanol facilities*; 2024, https://www.etipbioenergy.eu/value-chains/conversion-technologies/advanced-technologies/sugar-to-alcohols/flagship-first-of-a-kind-commercial-and-demonstration-cellulosic-ethanol-facilities.
(37) Humbird, D.; Davis, R.; Tao, L.; Kinchin, C.; Hsu, D.; Aden, A.; Schoen, P.; Lukas, J.; Olthof, B.; Worley, M. et al. *Process Design And Economics For Biochemical Conversion Of Lignocellulosic Biomass To Ethanol: dilute-Acid Pretreatment And Enzymatic Hydrolysis Of Corn Stover*; National Renewable Energy Laboratory (NREL), 2011.
(38) Aden, A.; Ruth, M.; Ibsen, K.; Jechura, J.; Neeves, K.; Sheehan, J.; Wallace, B.; Montague, L.; Slayton, A.; Lukas, J. *Process Design Report For Stover Feedstock: lignocellulosic Biomass To Ethanol Process Design And Economics Utilizing Co-Current Dilute Acid Prehydrolysis And Enzymatic Hydrolysis For Corn Stover*; National Renewable Energy Laboratory (NREL), 2002.
(39) Tullo, A. Braskem completes bioethylene expansion. *Chem. Eng. News* **2023**, *101* (25), 12.
(40) Frosi, M.; Tripodi, A.; Conte, F.; Ramis, G.; Mahinpey, N.; Rossetti, I. Ethylene from Renewable Ethanol: Process Optimization and Economic Feasibility Assessment. *J. Ind. Eng. Chem.* **2021**, *104*, 272−285.
(41) University of Pennsylvania. *Process Design for the Production of Ethylene from Ethanol*; 2012, https://repository.upenn.edu/cgi/viewcontent.cgi?article=1036&context=cbe_sdr.
(42) *Carbon Price Tracker*; 2024, https://ember-climate.org/data/data-tools/carbon-price-viewer/.
(43) *Global Average Levelised Cost of Hydrogen Production by Energy Source and Technology, 2019 and 2050 - Charts -Data & Statistics*; IEA, 2020. https://www.iea.org/data-and-statistics/charts/global-average-levelised-cost-of-hydrogen-production-by-https://www.iea.org/data-and-statistics/charts/global-average-levelised-cost-of-hydrogen-production-by-\protect\penalty-\@Menergy-source-and-technology-2019-and-2050.
(44) Strauss, W. *Global Wood Pellet Markets: 2023 in Review and Why Industrial Wood Pellets Are Key for the Future*; Canadian Biomass Magazine, 2024.
(45) Statista Research Department. Netherlands: Non-household electricity prices 2022. Statista, 2023; https://www.statista.com/statistics/596254/electricity-non-household-price-netherlands/.
(46) Danish Energy Agency. *Technology Data for Industrial Process Heat*; 2024. https://ens.dk/en/our-services/technology-catalogues/technology-data-industrial-process-heat.
(47) Deutz, S.; Bardow, A. Life-Cycle Assessment of an Industrial Direct Air Capture Process Based on Temperature-Vacuum Swing Adsorption. *Nat. Energy* **2021**, *6*, 203−213.
(48) Poluzzi, A.; Guandalini, G.; Guffanti, S.; Martinelli, M.; Moioli, S.; Huttenhuis, P.; Rexwinkel, G.; Palonen, J.; Martelli, E.; Groppi, G.; et al. Flexible Power and Biomass-To-Methanol Plants with Different Gasification Technologies. *Front. Energy Res.* **2022**, *9*, 795673.
(49) Rijksoverheid, *Gemeente Aa en Hunze Rapportage CO2-uitstoot*. 2024, https://klimaatmonitor.databank.nl/content/co2-uitstoot.
(50) *Cost Estimation Methodology for NETL Assessments of Power Plant Performance*; NETL, 2019.
(51) Peters, M. S.; Timmerhaus, K. D.; West, R. E. *Plant Design and Economics for Chemical Engineers*; McGraw-Hill, 2003.
(52) PBL Netherlands Environmental Assessment Agency. *Decarbonisation Options for Large Volume Organic Chemicals Production:*

https://doi.org/10.1021/acsomega.5c09670
ACS Omega 2026, 11, 4314−4332

SABIC Geleen; PBL Netherlands Environmental Assessment Agency, 2021. Accessed on: 26 May 2024.
(53) Nicholson, S. R.; Rorrer, N. A.; Carpenter, A. C.; Beckham, G. T. Manufacturing Energy and Greenhouse Gas Emissions Associated with Plastics Consumption. *Joule* **2021**, *5*, 673−686.
(54) Manfredi, S.; Tonini, D.; Christensen, T. H.; Scharff, H. Landfilling of waste: Accounting of greenhouse gases and global warming contributions. *Waste Manage. Res.* **2009**, *27*, 825−836.
(55) U.S. Environmental Protection Agency *Plastics and Climate Change: Numbers*; U.S. Environmental Protection Agency, 2010; Accessed: May 2024.
(56) Zimmermann, H.; Walzl, R. Ethylene. In *Ullmann's Encyclopedia of Industrial Chemistry*; Wiley, 2009.
(57) ICIS Europe. *Re-globalisation of PE prices and the challenges for 2023*; 2023, https://www.icis.com/asian-chemical-connections/2022/12/europe-re-globalisation-of-pe-prices-and-the-challenges-for-2023/, Accessed: 17 February 2025.
(58) ICIS. *Global polypropylene could also move from inflation to deflation in Q1 next year*; 2021, https://www.icis.com/asian-chemical-connections/2021/11/global-polypropylene-could-also-move-from-inflation-to-deflation-in-q1-next-year/. Accessed: 17 Februray 2025.
(59) Hamelinck, C. N.; van Hooijdonk, G.; Faaij, A. P. Ethanol from Lignocellulosic Biomass: Techno-Economic Performance in Short-, Middle- and Long-Term. *Biomass Bioenergy* **2005**, *28* (4), 384−410.

https://doi.org/10.1021/acsomega.5c09670
ACS Omega 2026, 11, 4314−4332